6-1-2013

Mimicking mesh refinement to construct initial data for a binary black hole system

Bradley James

Mimicking Mesh Refinement to Construct Initial Data for a Binary Black Hole System

by

Bradley W. James

Submitted to the School of Mathematical Sciences, College of Science

in partial fulfillment of the requirements for the degree of

Masters of Science in Applied and Computational Mathematics

at the

Rochester Institute of Technology

June 2013

Accepted by: Joshua A. Faber, School of Mathematical Sciences

Accepted by: Matthew J. Hoffman, School of Mathematical Sciences

Accepted by: John T. Whelan, School of Mathematical Sciences

Abstract

In order to perform an evolutionary calculation in General Relativity, accurate initial data is needed. A pseudospectral numerical method to solve both linear and nonlinear ordinary differential equations is introduced. We then calculate solutions to the Hamiltonian and momentum constraints for a binary black hole system utilizing such a pseudospectral method. The error resulting from the implementation is discussed at three locations in space: near the black holes, far from the black holes, and in between. A method to mimic mesh refinement through appropriate coordinate transforms is introduced with the result of lowering the maximum error in the system.

Contents

List of Figures

1 Introduction

To evolve a system in general relativity one must first obtain the initial data on a space like hypersurface, a generalization of the hyperplane, representing the initial time slice. The data must satisfy both the momentum constraints and the Hamiltonian constraint of general relativity. Once the initial data is obtained, an evolutionary calculation can be done. The majority of the methods commonly used at present to calculate the initial data, involve utilizing a pseudospectral method. Initial data in its native form is only C^2 at the location of the punctures, black holes, a problem when implementing a numerical solver that requires a function to be C^∞ on the interior of its domain.

This thesis begins by discussing the implementation of a general pseudospectral method to numerically solve both linear and nonlinear ordinary differential equations. A psuedospectral method involves first assuming the function for which we solve for is a finite sum of a group of basis functions, and then solving the equation exactly at a group of collocation points [3].

We then will examine a method of transforming the initial data so the punctures lie on the boundary of a closed compact domain [1]. This method involves a series of transformations which sends the Cartesian coordinates, denoted by (x, y, z) to a variation on the cylindrical coordinates, (A, B, ϕ). A pseudospectral method is then implemented in the new coordinates to solve the Hamiltonian constraint, a highly nonlinear equation of the form

$$\triangle u = f(u).$$

Two new transforms are discussed with the goal of lowering the overall error induced in the system. These transforms are made to mimic mesh refinement. The first sends points closer to the location of only one black hole while the second moves collocation points closer to both black holes. The result is a numerical method that lowers the error close to the location of the punctures while increasing the error as the distance from the punctures increases.

2 Pseuospectral Method for Ordinary Differential Equations

A differential equation can be written as

$$Lu(x) = f(x), \tag{2.1}$$

where L is a differential operator. The pseudospectral method for solving differential equations requires $u(x)$ to be written as an infinite sum over a set of basis functions, B_i, and then truncated after N terms

$$u(x) \approx u_N(x) = \sum_{i=0}^{N-1} c_i B_i(x). \tag{2.2}$$

Given coefficients $c_0, c_1, \ldots, c_{N-1}$, the residual is defined to be the difference between $Lu_N(x)$ and $f(x)$. If the residual is 0 for all x values then u_N is the exact solution to the original equation. Therefore, the pseudospectral method aims to minimize the residual of the differential equation

$$\min_{c_i} \quad Lu_N - f(x). \tag{2.3}$$

One way to minimize the residual function is to solve the equation exactly at a set of points known as collocation points. As the number of collocation points increases the difference between x_i and x_{i+1}, where x_i is the i^{th} collocation point, goes to 0 and the solution will be exact. The choice of collocation points and basis functions is important in optimizing convergence and can greatly speed up the rate of convergence of the pseudospectral

method.

2.1 Choosing A Basis

Making the correct choice of basis functions is extremely important. In almost all circumstances Chebyshev polynomials are the best choice of basis functions so they will be examined in this thesis. The Fourier cosine series has a basis defined by

$$F_n(\hat{x}) = \cos(n\hat{x}). \tag{2.4}$$

The change of variable defined by $\hat{x} = \arccos x$ results in the Chebyshev polynomials, denoted by $T_n(x)$,

$$T_n(x) = \cos(n \arccos(x)). \tag{2.5}$$

Since the Chebyshev polynomials are related to the Fourier cosine series through a change of variable, all the properties of a Fourier expansion hold for a Chebyshev expansion. Chebyshev polynomials do more than form a basis, they form an orthogonal basis. Therefore, given a function $f(x)$ the coefficients of the Chebyshev expansion can be solved using the inner product.

The Chebyshev polynomials satisfy a discrete orthogonality condition,

$$\sum_{k=0}^{N-1} T_i(x_k)T_j(x_k) = \begin{cases} 0 & i \neq j \\ N & i = j = 0 \\ \frac{N}{2} & i = j \neq 0 \end{cases}, \tag{2.6}$$

where

$$x_k = \cos\left(\frac{(2k+1)\pi}{2N}\right) \tag{2.7}$$

are the zeros of the N^{th} degree Chebyshev polynomial. The choice of the zeros of the N^{th} Chebyshev polynomials is made because this choice of collocation points minimizes the maximum value of the possible error between $u_N(x)$ and $u(x)$. It is important to note they do not necessarily minimize the overall error, but the maximum value the error can take. This is commonly known as the minimax principle. As stated in [3] "When in doubt, use Chebyshev polynomials ... Unless you're really, really sure that another set of basis functions is better, use Chebyshev polynomials."

If it is assumed that there is an expansion for $f(x)$

$$f(x) \approx \sum_{i=0}^{N-1} c_i T_i(x), \tag{2.8}$$

we can use Equation (2.6) to obtain an expression for the coefficients, c_i,

$$\sum_{k=0}^{N-1} f(x_k)T_j(x_k) = \sum_{k=0}^{N-1}\sum_{i=0}^{N-1} c_i T_i(x_k)T_j(x_k) = \begin{cases} 0 & i \neq j \\ c_i N & i = j = 0 \\ c_i \frac{N}{2} & i = j \neq 0 \end{cases}. \tag{2.9}$$

To solve for c_i, the result of Equation (2.9) is inverted to obtain

$$c_0 = \frac{1}{N}\sum_{k=0}^{N-1} f(x_k)T_0(x_k) = \frac{1}{N}\sum_{k=0}^{N-1} f(x_k), \tag{2.10}$$

$$c_j = \frac{2}{N}\sum_{k=0}^{N-1} f(x_k)T_j(x_k).$$

2.2 Linear Ordinary Differential Equations

Suppose we have the following linear ordinary differential equation we wish to solve:

$$a(x)u''(x) + b(x)u'(x) + c(x)u(x) = f(x); \qquad u(-1) = \alpha, \quad u(1) = \beta. \tag{2.11}$$

The boundary conditions imposed are Dirichlet boundary conditions with boundaries occurring at $x = \pm 1$. Only boundary conditions occurring at ± 1 are considered because the domain of the Chebyshev polynomials is $[-1, 1]$. If the boundary conditions are originally stated to occur at $a, b \in \mathbb{R}$ the equation can be rescaled appropriately to force the boundary to occur at ± 1.

Since the solution to the differential equation will be obtained through a pseudospectral method, $u(x)$ will be represented as

$$u(x) \approx \sum_{i=0}^{N-1} k_i T_i(x). \tag{2.12}$$

Substituting this representation for u into equation (2.11) the differential equation be-

comes

$$\sum_{i=0}^{N-1}(k_i(a(x)T_i''(x)+b(x)T_i'(x)+c(x)T_i(x)))=f(x), \tag{2.13}$$

with boundary conditions

$$\sum_{i=0}^{N-1}k_iT_i(-1)=\alpha,$$

$$\sum_{i=0}^{N-1}k_iT_i(1)=\beta. \tag{2.14}$$

In order to use the pseudospectral method we have to choose collocation points. The extrema of the $(N-1)^{\text{th}}$ degree Chebyshev polynomial minimize the maximum of the error in interpolation, therefore the choice of collocation points is

$$x_j=\cos\left(\frac{2j\pi}{2(N-1)}\right) \qquad j=0,1,2,\ldots,N-1.$$

In order to obtain a solution to (2.13), the equation will be solved exactly at the interior collocation points with boundary conditions imposed at $x=\pm1$. The coefficients therefore satisfy,

$$\sum_{i=0}^{N-1}(k_i(a(x_j)T_i''(x_j)+b(x_j)T_i'(x_j)+c(x_j)T_i(x_j)))=f(x_j), \tag{2.15}$$

for $j=1,2,\ldots,N-2$. Including the boundary conditions this is a system of N linear equations, one for each of the collocation points, and N unknowns, the coefficients of u_N. This system of equations can be represented as a linear system

$$A\vec{k} = \vec{f}(x).$$

Written explicitly,

$$\begin{bmatrix} 1 & -1 & 1 & \cdots & (-1)^{N-1} \\ A_{1,0} & A_{1,1} & A_{1,2} & \cdots & A_{1,N-1} \\ \vdots & & & \ddots & \vdots \\ A_{N-1,0} & A_{N-2,N-1} & A_{N-1,2} & \cdots & A_{N-2,N-1} \\ 1 & 1 & 1 & \cdots & 1 \end{bmatrix} \begin{bmatrix} k_0 \\ k_1 \\ \vdots \\ k_{N-2} \\ k_{N-1} \end{bmatrix} = \begin{bmatrix} \alpha \\ f(x_1) \\ \vdots \\ f(x_{N-2}) \\ \beta \end{bmatrix}. \quad (2.16)$$

The first and last rows of (2.16) implement the boundary conditions, namely $u(-1) = \alpha$ and $u(1) = \beta$. The interior terms of A are given by

$$A_{j,i} = a(x_j)T_i''(x_j) + b(x_j)T_i'(x_j) + c(x_j)T_i(x_j). \quad (2.17)$$

We can now solve (2.16) in a variety of fashions. One way is to calculate the inverse of A, then find the solution as $\vec{k} = A^{-1}\vec{f}(x)$. The problem with solving a linear equation in this fashion is in the computation of A^{-1} since it is a computationally intensive problem. Instead, Equation (2.16) is solved using LU factorization and reverse substitution.

2.3 Linear ODE Example

Consider the following linear ODE we wish to solve,

$$u''(x) - 3u'(x) + 2u(x) = e^x; \qquad u(-1) = 2e^{-1} + e^{-2}, \quad u(1) = e^2. \tag{2.18}$$

The solution obtained analytically is

$$u(x) = (1 - x)e^x + e^{2x}.$$

In order to determine the error 100 evenly spaced points are chosen between -1 and 1. The error is then the L_2 norm i.e., the square root of the sum of the squares, of the spacing between the interpolated solution and the known solution. Using the pseudospectral method described in the previous section, exponential convergence towards the solution is obtained, Figure 1.

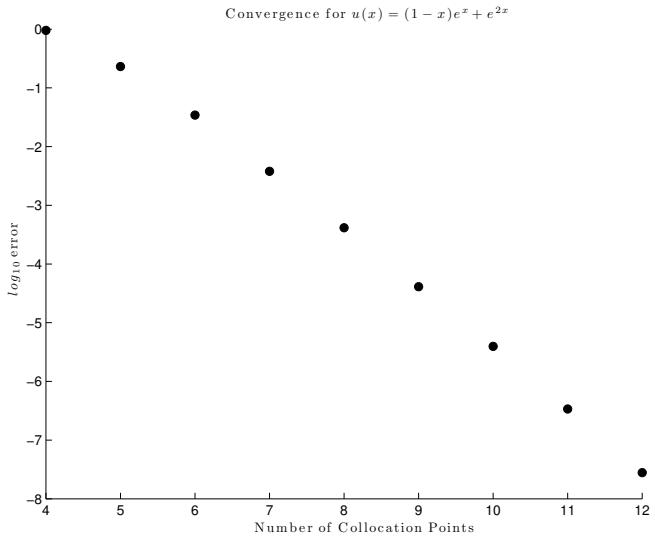

Figure 1: Plot showing exponential convergence for $u'' - 3u' + 2u = e^x$ with initial conditions $u(-1) = 2e^{-1} + e^{-2}$ and $u(1) = e^2$. Extrapolating, we see that only 20 collocation points or so are required to reach the double precision roundoff noise limit of 10^{-16}

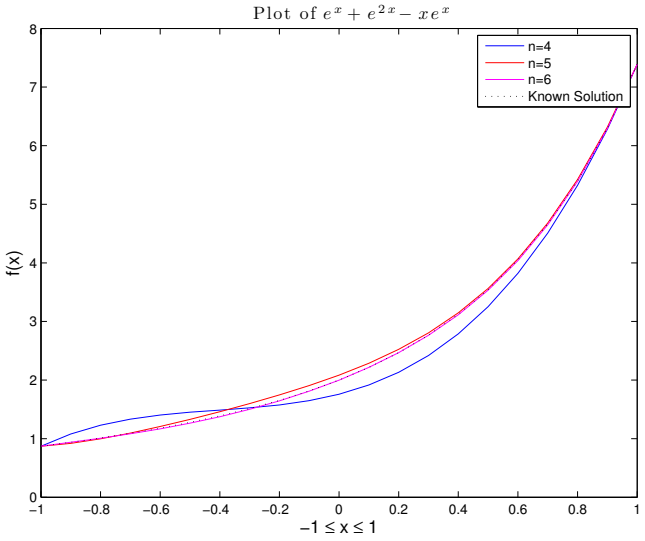

Figure 2: A visualization of $n = 4$, $n = 5$, $n = 6$, and the known solution using a pseudospectral method.

2.4 Nonlinear Ordinary Differential Equations

For the purposes of demonstrating how to solve a nonlinear ordinary differential equation we will assume that the equation is of the following form,

$$a(x)u''(x) + b(x)u'(x) + u(x)^2 = f(x); \qquad u(-1) = \alpha, \quad u(1) = \beta. \tag{2.19}$$

As in the linear case, Dirichlet boundary conditions are imposed at 1 and -1. Since a pseudospectral method is being utilized to solve the nonlinear ODE, the solution is assumed to take the form

$$u(x) \approx \sum_{i=0}^{N-1} k_i T_i(x) \tag{2.20}$$

Substituting the representation of u into equation (2.19),

$$\sum_{i=0}^{N-1} k_i \left(a(x)T_i''(x) + b(x)T_i'(x)\right) + \left(\sum_{i=0}^{N-1} k_i T_i(x)\right)^2 = f(x). \tag{2.21}$$

The extrema of the $(N-1)^{th}$ degree Chebyshev polynomial are used as collocation points. In the case of a linear ordinary differential equation the system could be written linearly as $A\vec{k} = \vec{f}(x)$. The nonlinear $u^2(x)$ term prevents Equation (2.21) from being written in such a form, instead the resulting equation will be solved using Multivariate Newton's Method, defined iteratively as

$$\vec{k}_{n+1} = \vec{k}_n - J^{-1}\vec{F}_n,$$

where J is the Jacobian matrix whose elements take the form:

$$\frac{\partial A}{\partial k_i} = a(x)T_i''(x) + b(x)T_i'(x) + 2\left(\sum_{i=0}^{N-1} T_i(x)\right) T_i(x)$$

and F_n is

$$\vec{F}_n = \begin{pmatrix} F_n^0 \\ \vdots \\ F_n^m \\ \vdots \\ F_n^{N-1} \end{pmatrix}.$$

$$\vec{F}_n^0 = \sum_{i=0}^{N-1} k_{i,n} T_i(-1) - \alpha,$$

$$\vec{F}_n^{N-1} = \sum_{i=0}^{N-1} k_{i,n} T_i(1) - \beta, \tag{2.22}$$

$$\vec{F}_n^m = \sum_{i=0}^{N-1} k_{i,n}(a(x_m)T_i''(x_m) + b(x_m)T_i'(x_m)) + \left(\sum_{i=0}^{N-1} k_{i,n} T_i(x_m)\right)^2 - f(x_m).$$

The first and last rows of $\vec{F}$ implement the boundary conditions. The middle rows of $\vec{F}$ require the differential equation to be solved at the collocation points. If an exact solution is found using Newton's Method it will be the case that $\vec{F} = \vec{0}$. In general the method is run until $||\vec{k}_n - \vec{k}_{n-1}||_2 < \epsilon$, where ϵ is the acceptable error tolerance.

2.5 Nonlinear ODE Example

Suppose we have the following nonlinear differential equation to solve,

$$u''(x) - u(x)^2 = e^x - e^{2x}; \qquad u(-1) = e^{-1}, \quad u(1) = e. \tag{2.23}$$

Analytically the solution is obtained as

$$u(x) = e^x.$$

The error is the L_2 norm of the difference between the interpolated solution of a given number of collocation points and the known solution at 100 evenly spaced points. Using the

psuedospectral method described previously, exponential convergence towards the solution is obtained, Figure 3.

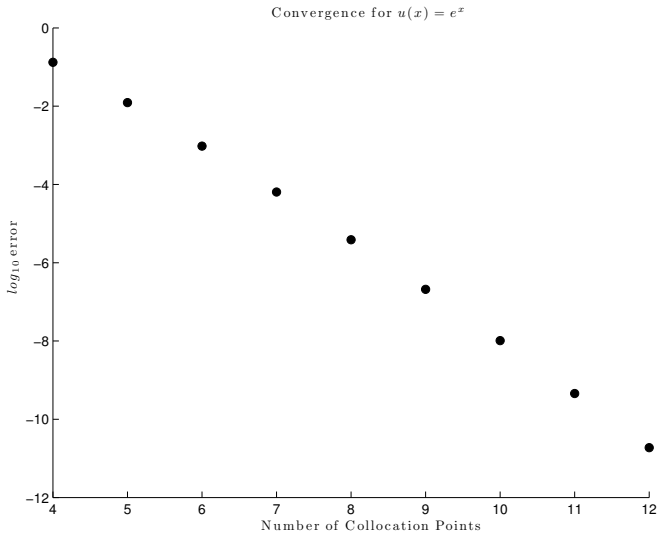

Figure 3: Plot showing exponential convergence for $u'' - u^2 = e^x - e^{2x}$ with initial conditions $u(-1) = e^{-1}$ and $u(1) = e$.

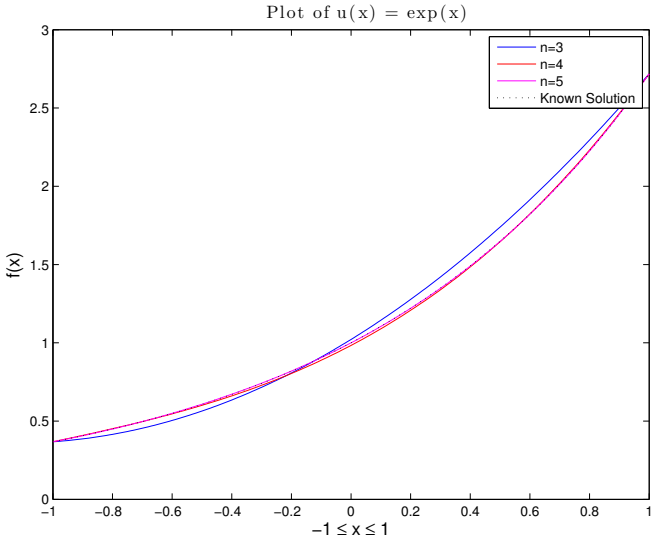

Figure 4: A visualization for $n = 3$, $n = 4$, $n = 5$, and the known solution using a pseudospectral method.

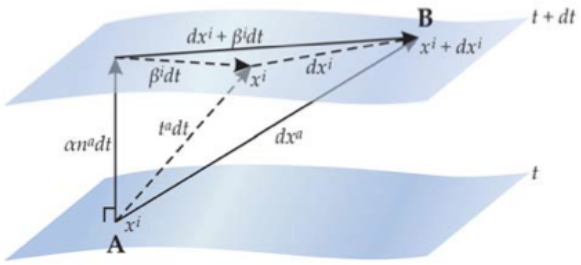

Figure 5: A diagram showing the various elements of the metric. Reproduced from [2].

3 The Hamiltonian and Momentum Constraints

In what follows we will set up the problem for solving the initial data for a binary black hole system (a system with two black holes). The metric takes the conformally flat form

$$g_{\mu\nu} \equiv (-\alpha^2 + \beta_i\beta^i)\mathrm{d}t^2 + 2\beta_i \mathrm{d}t\mathrm{d}x^i + \hat{\gamma}_{ij}\mathrm{d}x^i\mathrm{d}x^j,$$

where α is the lapse function, β the shift vector, and $\hat{\gamma}_{ij}$ the spatial three metric intrinsic to a hypersurface [5]. The lapse function measures the distance in time between successive hypersurfaces (moments in time) along a time-like curve perpendicular to the spatial hypersurface. The shift vector measures the distance between traveling along the unit normal perpendicular to the spatial slice and traveling with stationary spatial coordinates. For consistency and simplicity the two black holes will be located at $x = \pm b$, $y = 0$, and $z = 0$.

The binary black hole initial data problem has four constraints, three momentum constraints and the Hamiltonian constraint. If the physical extrinsic curvature, $\hat{K}^{ab}$ is scaled by

a conformal factor[1], ψ, the conformal extrinsic curvature, K is obtained with $K^{ab} = \psi^2 \hat{K}^{ab}$. It follows that the momenta constraints can be written as[2]

$$\nabla_a K^{ab} = 0. \tag{3.1}$$

The momentum constraints can be thought of as a generalized divergence. The Bowen-York solution to the momentum constraints for two black holes with given momentums P_1^a, P_2^a and spins S_1^a, S_2^a, is

$$K_{ab} = \sum_{k=1}^{N_{BH}} \frac{3}{2r_k^2}(P_k^a n_k^b + P_k^b n_k^a - (\gamma^{ab} - n_k^a n_k^b)(P_k \cdot n_k)) + \frac{3}{r_k^3}((\vec{S}_k \times \vec{n}_k)^a n_k^b + (\vec{S}_k \times \vec{n}_k)^b n_k^a) \tag{3.2}$$

where N_{BH} is the number of black holes, r_i is the distance to black hole $i \in \{1, 2\}$

$$r_{1,2} = \sqrt{(x \pm b)^2 + y^2 + z^2},$$

n_i^a is the radial unit normal vector, defined as x^a / r_i, and γ is the conformal three metric (in our case equivalent to the identity matrix).

The Hamiltonian constraint is

$$\triangle \psi + \frac{1}{8} K^{ab} K_{ab} \psi^{-7} = 0 \tag{3.3}$$

[1] ψ factors the determinant of the spatial 3-metric, $\hat{\gamma}$, such that $\psi = [\det(\hat{\gamma}_{ij})]^{\frac{1}{12}}$. The conformal 3-metric, γ, is defined by $\gamma = \psi^{-4} \hat{\gamma}_{ij}$.

[2] For an explanation of notation see appendix B

with boundary conditions $\psi \to 1$ as $r \to \infty$. A solution to the Hamiltonian constraint is sought in order to generate initial data for an evolutionary calculation.

4 The Auxiliary Function

The solution for the conformal factor, ψ, is known to be singular at the location of the black holes [1]. In order to obtain the maximum convergence possible ψ is decomposed into its singular and nonsingular pieces,

$$\psi = u + \sum_{i=1}^{N_{BH}} \frac{m_i}{2r_i}, \tag{4.1}$$

where N_{BH} is the number of black holes and m_i is the i^{th} puncture mass. Using this break down, u is a regular function, finite, and continuous everywhere. Since $\psi \to 1$ as $r \to \infty$ the new boundary condition is, $u \to 1$ as $r \to \infty$. It is numerically easier to solve a problem with boundary conditions that approach 0 as $r \to \infty$. Therefore the boundary condition will be restated as $u - 1 \to 0$ as $r \to \infty$.

We now wish to write the Hamiltonian constraint in terms of the new variable u. This process is outlined in [4]. First, the following variables are defined

$$\frac{1}{\alpha} = \sum_{i=1}^{N_{BH}} \frac{m_i}{2r_i}, \tag{4.2}$$

and

$$\beta = \frac{1}{8}\alpha^7 K^{ab} K_{ab}. \tag{4.3}$$

The Hamiltonian constraint can now be written in terms of α, β, and u. Since $\sum_{i=1}^{N_{BH}} \frac{m_i}{2r_i}$

has zero Laplacian, $\triangle u = \triangle \psi$. Substituting the representation of ψ into the Hamiltonian constraint, equation (3.3),

$$\triangle u + \frac{1}{8} K^{ab} K_{ab} \left(u + \frac{1}{\alpha} \right)^{-7} = 0.$$

Multiplying the equation by α^7/α^7, the constraint equation becomes

$$\triangle u + \beta (1 + \alpha u)^{-7} = 0. \tag{4.4}$$

This is the version of the Hamiltonian constraint which will be numerically solved. Once a solution for u has been obtained the solution for the conformal factor, ψ, follows trivially by equation (4.1).

5 Compactification

Black hole initial data is not continuously differentiable at the location of the punctures (black holes). In order to obtain exponential convergence for a numerical solution a continuously differentiable function on the interior of the domain is required. In addition the entire space of (x, y, z) should be represented as a compact rectangular domain. For this reason the compactification scheme presented in [1] is introduced. The idea behind the compactification scheme is to send the two black holes, located at $x = \pm b$, to the boundary of a rectangular grid. The final result is a transform that sends (A, B, ϕ), a variation of the cylindrical coordinates, to (x, y, z). This is done through a series of transformations

$$(A, B, \phi) \to (\xi, \eta, \phi) \to (X, R, \phi) \to (x, \rho, \phi) \to (x, y, z). \tag{5.1}$$

We will first start with the cylindrical coordinates, (x, ρ, ϕ), such that

$$x = x, \qquad y = \rho \cos \phi, \qquad z = \rho \sin \phi, \qquad \phi \in [0, 2\pi]. \tag{5.2}$$

We will now combine x and ρ to form c,

$$c = x + \mathrm{i}\rho. \tag{5.3}$$

We now wish to do two things

- Map lines to circles
- Map the line connecting the two black holes to the unit circle

This can be done by applying the Joukowsky transform defined by

$$c = \frac{b}{2}(C + C^{-1}), \qquad \text{where } C = X + \mathrm{i}R. \tag{5.4}$$

The two black holes, previously located at $x = \pm b$ are now located at $C = \pm 1$.

To explain the next steps a digression will be made by first discussing a transformation which makes the distances regular in a two dimensional plane. In making the distances regular, regularity of u is also obtained at the location of the punctures. As above, consider the mapping

$$c_2 = C_2^2$$

where $c_2 = x + iy$ and $C_2 = X + iY$. The old coordinates are (x, y) and the new coordinates are (X, Y). The distance in (X, Y) becomes regular at the location of the punctures

$$\sqrt{x^2 + y^2} = C\bar{C} = X^2 + Y^2.$$

We will now show the distance in (5.4) is regular in three dimensions. Since the black holes are located at $x = \pm b$ they are also located at $c = \pm b$. It is fairly easy to see the distances to the black holes are $r_{1,2} = |c \mp b|$. In the (X, R) coordinates this becomes

$$
\begin{aligned}
r_{1,2} &= |c \mp b| \\
&= |\frac{b}{2}((X + \mathrm{i}R)^2 + 1 \mp b)| \\
&= \frac{b}{2\sqrt{X^2 + R^2}} \sqrt{(X^2 - R^2 \mp X + 1)^2 + (2RX \mp 2R)^2} \\
&= \frac{b}{2\sqrt{X^2 + R^2}} \left((X \mp 1)^2 + R^2\right).
\end{aligned}
$$

This is regular at the location of the two punctures, i.e $C = \pm 1$.

Since we have now achieved regularity at the location of the two punctures. We now wish to map a compact rectangular region onto the (X, R) plane. This can be achieved in the following way:

$$
C = e^{\zeta}, \qquad \zeta = \xi + \mathrm{i}\eta, \qquad \xi \in [0, \infty), \qquad \eta \in [0, \pi]. \tag{5.5}
$$

Substituting the new representation for C into equation (5.4) we obtain,

$$
\begin{aligned}
c &= \frac{b}{2}(e^{\zeta} + e^{-\zeta}) \\
&= b \cosh \zeta.
\end{aligned} \tag{5.6}
$$

Recall from equation (5.3) that $c = x + \mathrm{i}\rho$, therefore $x = \mathrm{Re}(b \cosh \zeta)$ and $\rho = \mathrm{Im}(b \cosh \zeta)$. We can now obtain expressions for x and ρ in terms of ξ and η,

$$x = b\cosh\xi\cos\eta, \qquad \rho = b\sinh\xi\sin\eta. \tag{5.7}$$

To compactify the coordinates from $(-\infty, \infty)$ to $(-1, 1)$ arctanh and arctan are used. Choosing

$$\xi = 2\text{arctanh}A, \qquad \eta = \frac{\pi}{2} + 2\arctan B. \tag{5.8}$$

To get the compact form for x, y, and z several properties of $\cosh(x)$ and $\sinh(x)$ are needed:

$$\cosh^2(x) = \frac{1}{1-\tanh^2(x)}, \qquad \sinh^2(x) = \frac{\tanh^2(x)}{1-\tanh^2(x)}$$
$$\cosh(2x) = \cosh^2(x) + \sinh^2(x), \qquad \sinh(2x) = 2\cosh(x)\sinh(x).$$

Using the above properties the following can be determined:

$$\begin{aligned}
\cosh(\xi) &= \cosh^2(\text{arctanh}(A)) + \sinh^2(\text{arctanh}(A)) = \frac{1+A^2}{1-A^2}, \\
\sinh(\xi) &= 2\sqrt{\cosh^2(\text{arctanh}(A))\sinh^2(\text{arctanh}(A))} = \frac{2A}{1-A^2}, \\
\cos(\eta) &= \cos\left(\frac{\pi}{2} + 2\arctan(B)\right) = -2\sin(\arctan(B))\cos(\arctan(B)) = \frac{-2B}{1+B^2}, \\
\sin(\eta) &= \sin\left(\frac{\pi}{2} + 2\arctan(B)\right) = \cos^2(\arctan(B)) - \sin^2(\arctan(B)) = \frac{1-B^2}{1+B^2}.
\end{aligned} \tag{5.9}$$

In summary we can define the map from (A, B, ϕ) to (x, y, z) by

$$x = b\frac{A^2+1}{A^2-1}\frac{2B}{1+B^2},$$
$$y = b\frac{2A}{1-A^2}\frac{1-B^2}{1+B^2}\cos\phi, \tag{5.10}$$
$$z = b\frac{2A}{1-A^2}\frac{1-B^2}{1+B^2}\sin\phi.$$

The black holes are successfully moved to the boundary and are located at $(0, \pm 1, \phi)$, occupying edges of the box in the (A, B, ϕ) coordinates, shown in Figure **??**. Using the new coordinates we can now numerically solve for u.

To convert from (x, y, z) to (A, B, ϕ) we use the relations defined in appendix C .

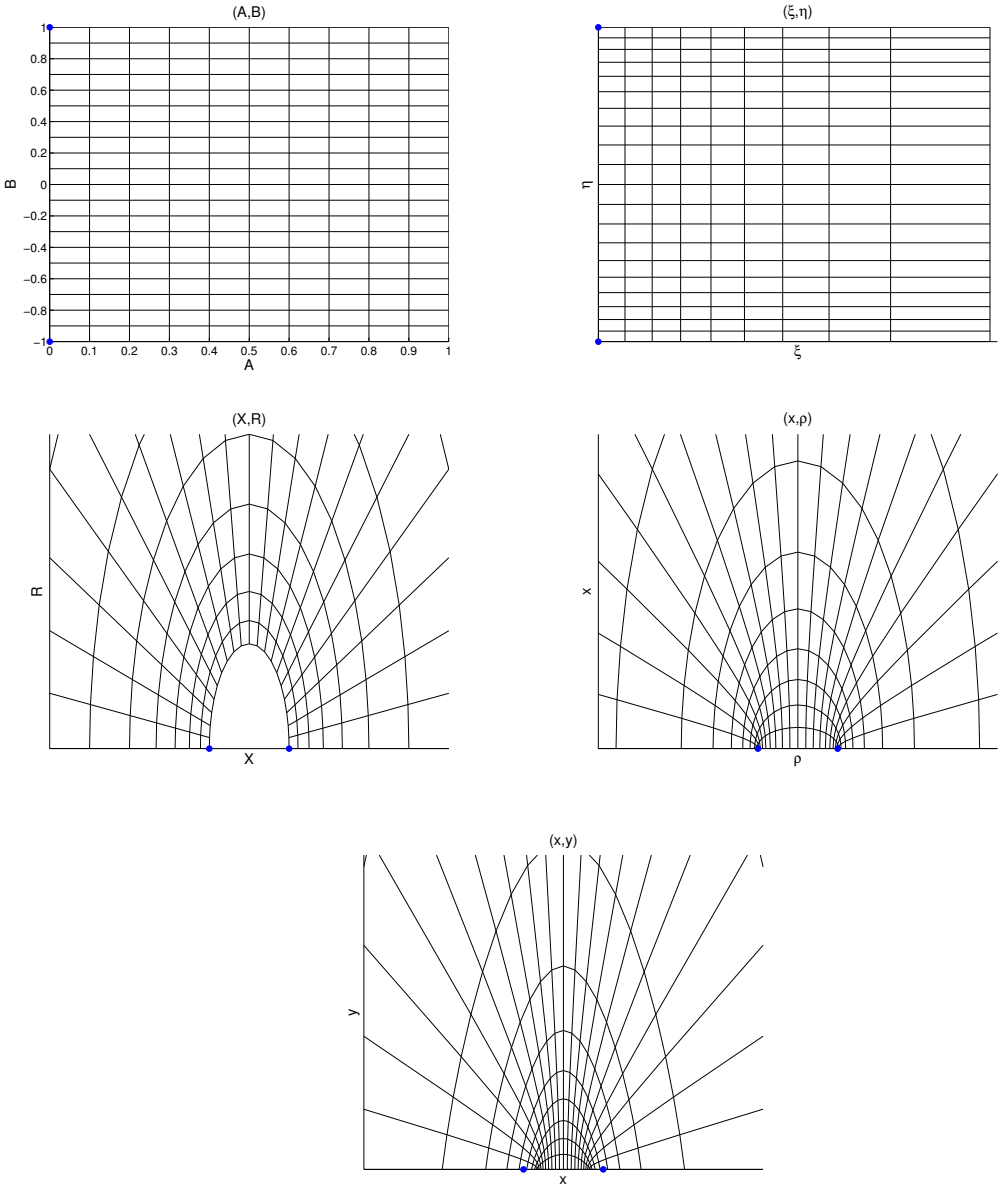

Figure 6: Reading top left to right, a 2-D slice of the different transforms to go from the (A, B, ϕ) coordinates to the Cartesian coordinates. The dots (blue) represent the location of the black holes in each coordinate system.

6 Obtaining A Numerical Solution

We will now discuss how to obtain a numerical solution to the Hamiltonian constraint for u, and hence ψ, through use of a pseudospectral method. Recall that the Hamiltonian constraint is

$$\triangle u + \beta(1 + \alpha u)^{-7} = 0.$$

Since we will be solving the equation in the (A, B, ϕ) coordinates the Laplacian must be determined in the new coordinates. It can be written in the form

$$\triangle = L_{AA}\frac{\partial^2}{\partial A^2} + L_A\frac{\partial}{\partial A} + L_{BB}\frac{\partial^2}{\partial B^2} + L_B\frac{\partial}{\partial B} + L_{\phi\phi}\frac{\partial^2}{\partial \phi^2}, \tag{6.1}$$

where the individual terms are given by

$$F = b^2[(A^4+1)(B^2-1)^2 + 2A^2(B^4+6B^2+1)], \tag{6.2}$$

$$L_{AA} = \frac{1}{4}\frac{(A^2-1)^4(1+B^2)^2}{F}, \tag{6.3}$$

$$L_A = \frac{L_{AA}}{A}, \tag{6.4}$$

$$L_{BB} = \frac{1}{4}\frac{(A^2-1)^2(1+B^2)^4}{F}, \tag{6.5}$$

$$L_B = \frac{2BL_{BB}}{B^2-1}, \tag{6.6}$$

$$L_{\phi\phi} = \frac{1}{4b^2}\frac{(B^2+1)^2(A^2-1)^2}{A^2(B^2-1)^2}. \tag{6.7}$$

A pseudospectral method will be employed to solve for u. u will be expanded into Chebyshev polynomials in the A and B directions and Fourier nodes in the ϕ direction,

$$u(A,B,\phi) \approx \sum_{i=0}^{N_A-1} \sum_{j=0}^{N_B-1} \sum_{k=0}^{N_\phi-1} c_{ijk} \bar{T}_i(A) T_j(B) F_k(\phi), \tag{6.8}$$

where $T_j(x)$ is the j^{th} Chebyshev polynomial, $\bar{T}_i(x) = T_i(2x-1)$ is the same polynomial as $T_i(x)$ defined on $[0,1]$, and $F_k(\phi)$ are orthogonal trigonometric functions that we define as

$$F_k(\phi) = \begin{cases} \sin(|k'|\phi) & k' < 0 \\ \cos(k'\phi) & k' \geq 0 \end{cases} \qquad k' = k - \frac{N_\phi}{2}. \tag{6.9}$$

We evaluate $\bar{T}_i(x)$ in the A direction instead of $T_i(x)$ because A is defined between $[0,1]$. We now wish to solve equation (3.3) using the approximation of $u(A,B,\phi)$ in equation (6.8) for the $N = N_A \times N_B \times N_\phi$ coefficients c_{ijk}. The approximation for u is evaluated at N collocation points defined on a rectangular grid. In the setup there is no boundary in the ϕ direction and the boundary points in the B direction are ignored since they represent a coordinate boundary rather than a physical one. There is a boundary at $A = 1$ with $u(A=1) = 0$. The collocation points in the A and B directions are chosen to be

$$A_i = \frac{1}{2} \cos\left(\frac{(i+1)\pi}{N_A - 1} + 1 \right), \qquad 0 \leq i \leq N_A - 1, \tag{6.10}$$

$$B_j = \cos\left(\frac{2j-1}{2N_B} \right), \qquad 0 \leq j \leq N_B - 1. \tag{6.11}$$

For the ϕ direction we choose

$$\phi_k = \frac{2\pi k}{N_\phi}. \tag{6.12}$$

7 Measuring Error

A method of describing the error will now be discussed. One problem that presents itself while measuring the error, outside of numeric solutions, is that there is no known solution for u nor ψ. One way to obtain an error measure is to compare Laplacian, obtained using a fourth order stencil, with the solution obtained from $\beta(1+\alpha u)^{-7}$. The stencil for a second derivative in 2-D is given by the following coefficients.

$$\frac{1}{h^2}\begin{pmatrix} 0 & 0 & -\frac{1}{12} & 0 & 0 \\ 0 & 0 & \frac{4}{3} & 0 & 0 \\ -\frac{1}{12} & \frac{4}{3} & -\frac{15}{2} & \frac{4}{3} & -\frac{1}{12} \\ 0 & 0 & \frac{4}{3} & 0 & 0 \\ 0 & 0 & -\frac{1}{12} & 0 & 0 \end{pmatrix} \tag{7.1}$$

If the Hamiltonian constraint, Equation (4.4), is solved perfectly then $\triangle u = -\beta(1+\alpha u)^{-7}$ for all (x, y, z). The expected result is something that resembles Figure 7. The error is smaller closer to the collocation points, and on a collocation point the error is 0. For this reason we will look at a grid of points; if we only looked at one point on the grid then the error could be greatly affected by how close it is to a collocation point for a given N_A, N_B, N_ϕ. We will also examine the total error over the range numerically by using the L_2 norm.

Grids will be examined in three different regions on the plane. The two blacks holes will be located at $(\pm\frac{1}{2}, 0, 0)$. The first region is close to the black holes. For our purposes we define close as being a distance of less than 0.3 away from either black hole. Recall that the distance between the two black holes is 1. In this area there is the greatest error in the numerical solver.

Figure 7: The expected shape of the error. At collocation points, the error goes to zero, and oscillates with decreasing amplitude as we move further from the black hole.

The next area to examine is far away from the black holes. This is defined as the area where the distance from either black hole is at least 0.7. At this distance the solutions should be almost exact because u is going towards the boundary condition of 1. The last region is the middle region which is simply the area between the two previous regions. Through examining the error in these regions we will build an additional transform which will work towards lowering the overall error in the system.

Four examples will now be shown. The goal of these cases is to show the versatility of the method for different spins, momenta, and mass. In all diagrams of the error the near section will be a line of points from $x = -0.75$ to $x = 0.75$, $y = 0.01$, and $z = 0.01$; the middle section will be a line at $x = 0.05$, $y = 0.05$, and $z = -0.25$ to $z = 0.25$; the far

section will be at $x = -0.75$ through $x = 0.75$, $y = 0.5$, and $z = 0.5$.

8 Examples

We will now discuss multiple examples through varying spin, momentum and mass of the black holes. The first black hole is located at $x = 0.5$, $y = 0$, $z = 0$ and the second black hole at $x = -0.5$, $y = 0$, $z = 0$. This determination is made so the distance between the two black holes is one.

8.1 Example 1

We will first examine a case in which both black holes have equal mass and linear momenta P_{y1} and P_{y2}.

$$m_1 = m_2 = \frac{1}{3}$$

$$P_1 = (0, P_{y1}, 0), \qquad P_2 = (0, P_{y2}, 0)$$

$$S_1 = S_2 = \vec{0}.$$

For this example the extrinsic curvature, K_{ab}, and its contraction will be obtained analytically. In the other examples this will not be done. Using Equation (3.2) we find that

$$K_{ab} = \begin{pmatrix} K_{11} & K_{12} & K_{13} \\ K_{21} & K_{22} & K_{23} \\ K_{31} & K_{32} & K_{33} \end{pmatrix}$$

with the individual terms given by

$$
\begin{aligned}
K_{11} &= \frac{3y_1P_{y1}}{r_1^4}\left(\left(\frac{x_1}{r_1}\right)^2-1\right)+\frac{3y_2P_{y2}}{r_2^4}\left(\left(\frac{x_2}{r_2}\right)^2-1\right),\\
K_{21}=K_{12} &= \frac{3}{r_1^2}\left(P_{y1}\frac{x_1}{r_1}+\frac{x_1y_1^2P_{y1}}{r_1^3}\right)+\frac{3}{r_2^2}\left(P_{y2}\frac{x_2}{r_2}+\frac{x_2y_2^2P_{y2}}{r_2^3}\right),\\
K_{31}=K_{13} &= \frac{3x_1z_1y_1P_{y1}}{r_1^5}+\frac{3x_2z_2y_2P_{y2}}{r_2^5},\\
K_{22} &= \frac{3P_{y1}y_1}{r_1^3}\left(1+\frac{y_1^2}{r_1^2}\right)+\frac{3P_{y2}y_2}{r_2^3}\left(1+\frac{y_2^2}{r_2^2}\right),\\
K_{32}=K_{23} &= \frac{3}{r_1^2}\left(\frac{z_1P_{y1}}{r_1}+\frac{x_1y_1z_1P_{y1}}{r_1^3}\right)+\frac{3}{r_2^2}\left(\frac{z_2P_{y2}}{r_2}+\frac{x_2y_2z_2P_{y2}}{r_2^3}\right),\\
K_{33} &= \frac{3}{r_1^2}\left(\frac{z_1^2}{r_1^2}-1\right)\frac{y_1P_{y1}}{r_1}+\frac{3}{r_2^2}\left(\frac{z_2^2}{r_2^2}-1\right)\frac{y_2P_{y2}}{r_2}.
\end{aligned}
$$

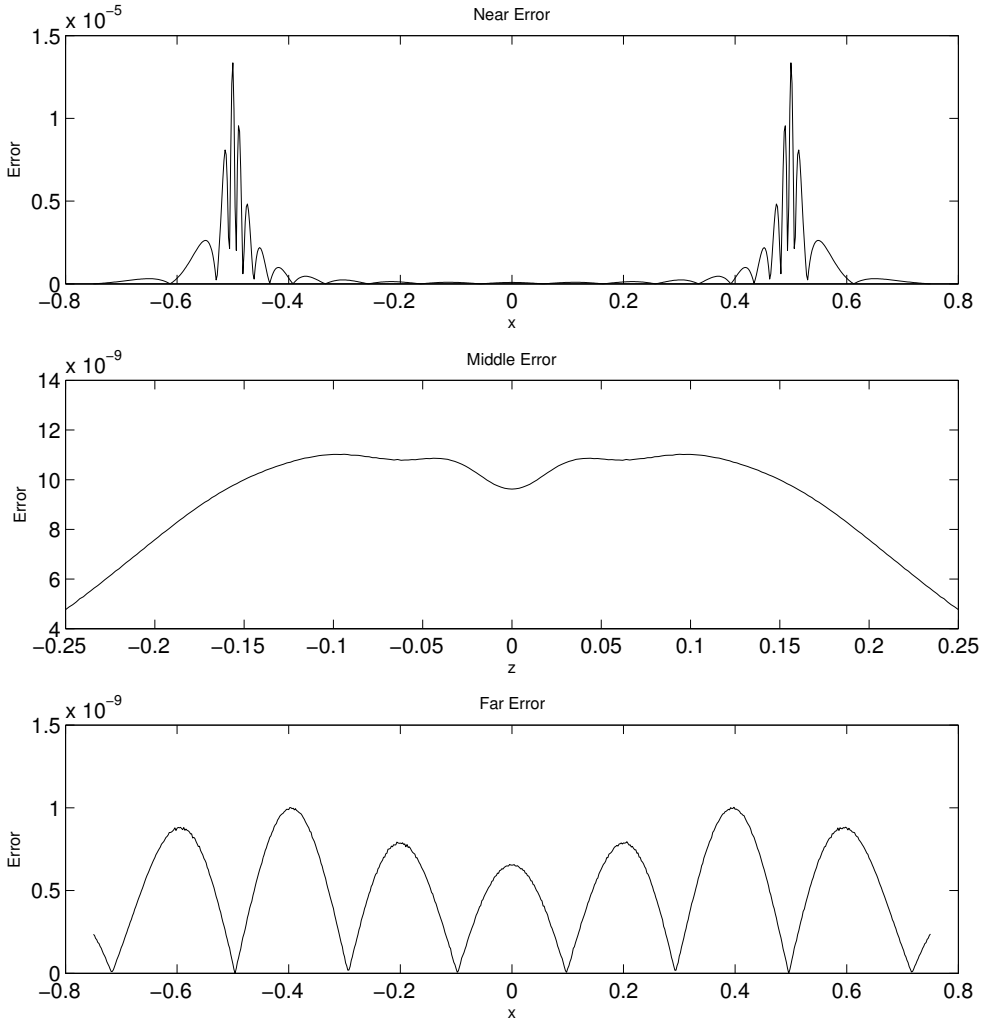

Figure 8: The error for a binary black hole system with $m_1 = m_2 = \frac{1}{3}$, $P_1 = (0, 0.05, 0)$, $P_2 = (0, -0.05, 0)$, $S_1 = S_2 = \vec{0}$.

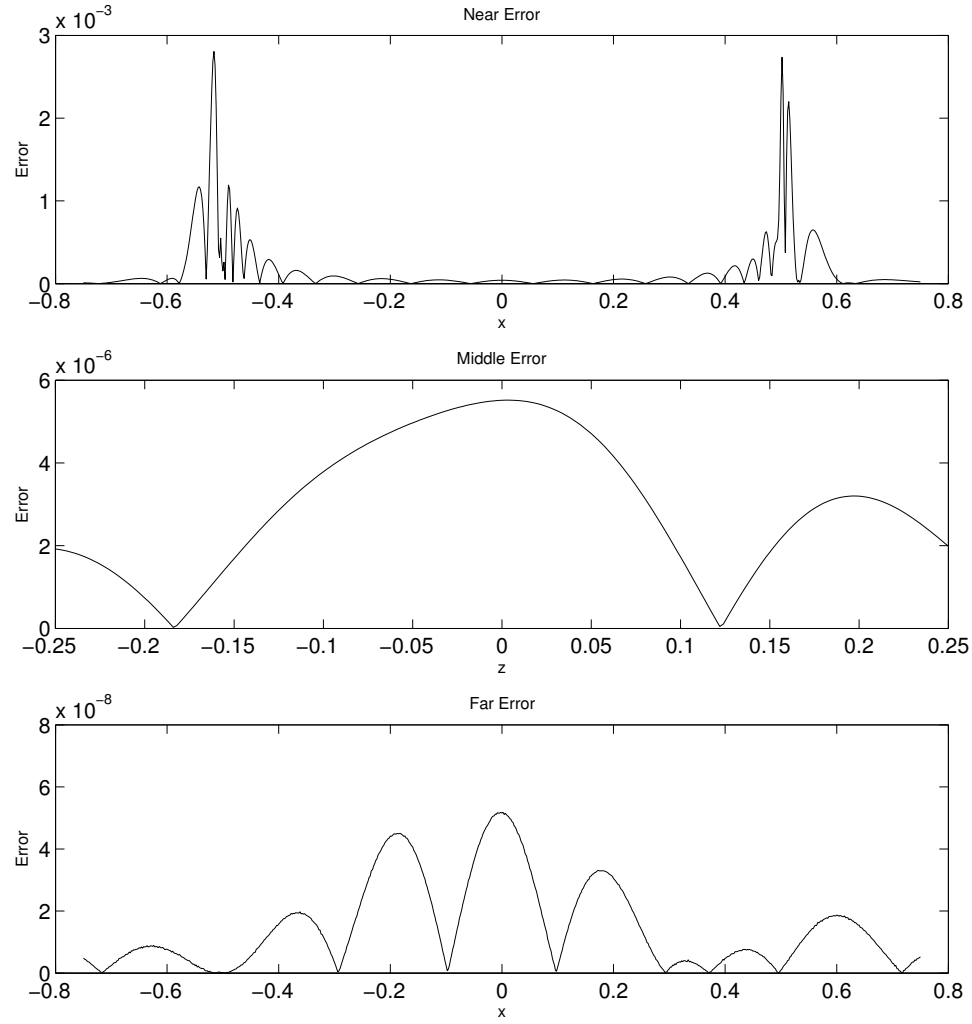

Figure 9: The error for a binary black hole system with $m_1 = m_2 = \frac{1}{3}$, $P_1 = (0, 0.05, 0)$, $P_2 = (0, -0.05, 0)$, $S_1 = (0.03, 0.03, 0.03)$, $S_2 = (0, 0, 0.05)$.

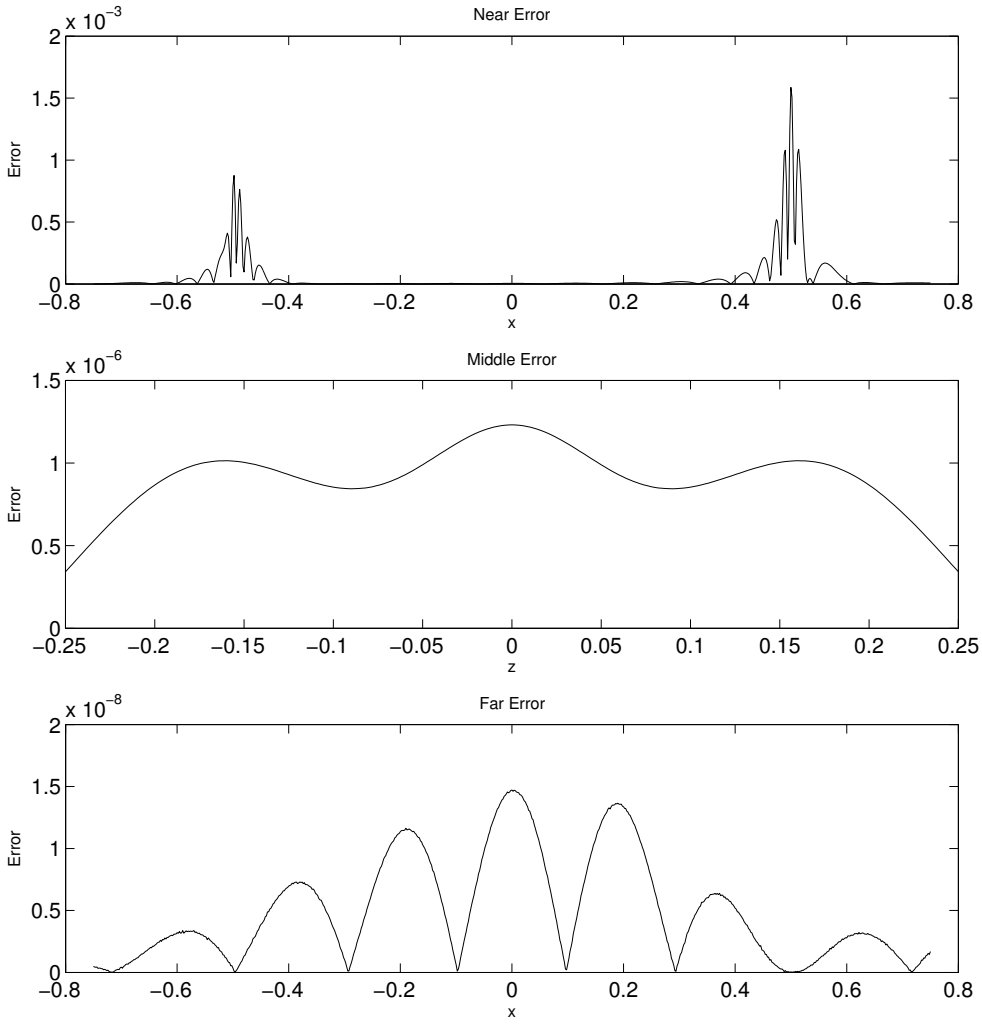

Figure 10: The error for a binary black hole system with $m_1 = 0.4$, $m_2 = 0.1$, $P_1 = (0, 0.05, 0)$, $P_2 = (0, -0.05, 0)$, $S_1 = (0, 0, 0.05)$, $S_2 = \vec{0}$.

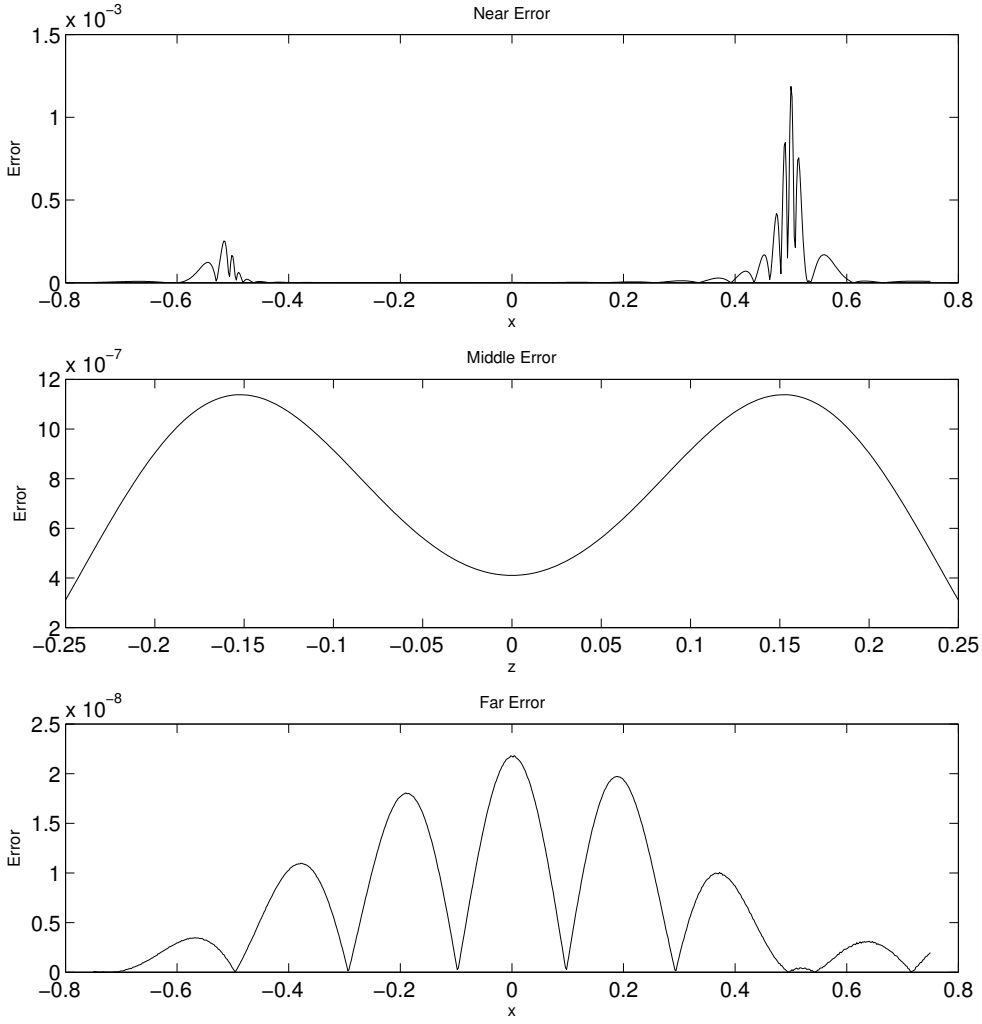

Figure 11: The error for a binary black hole system with $m_1 = 0.4$, $m_2 = 0.1$, $P_1 = P_2 = \vec{0}$, $S_1 = (0, 0, 0.05)$, $S_2 = \vec{0}$.

In all of the error diagrams the same number of collocation points are used, therefore the same collocation points are being used. This will not be the case when we examine the additional transforms even though the same number of collocation points will be used. There is already some bias introduced in the collocation points for them to be closer to the black holes because the collocation points are chosen to be the zeros of the $n + 1^{\text{st}}$ degree Chebyshev polynomial which concentrates points close to the endpoints.

In all of the cases the error is the least in the section of the grid designated as far. In all of the cases of equal mass black holes the error behaves as expected for the middle and near errors. The error is the largest close to the black hole and decreases as we move away from the black hole (minus the variations caused by the proximity of collocation points).

In order to remedy some of these errors we will introduce two transforms which will shift collocation points closer to the black holes in a fashion that will lower the overall error of the system.

9 Mimicking Mesh Refinement Through Additional Transforms

The idea behind an additional transform is to mimic mesh refinement. Rather than performing domain splitting to vary the resolution of our spectral method, an additional transform will be used. We will consider mappings defined by parameters c_A and c_B and maps $f : A \to \hat{A}$ and $g : B \to \hat{B}$ such that f maps $[0, 1]$ to $[0, 1]$ in a smooth one-to-one fashion and g does the same on $[-1, 1]$. In order to solve the Hamiltonian constraint the mapping does not need to be invertible; however we wish to find the solution at a given (x, y, z) coordinate so we will only consider invertible maps.

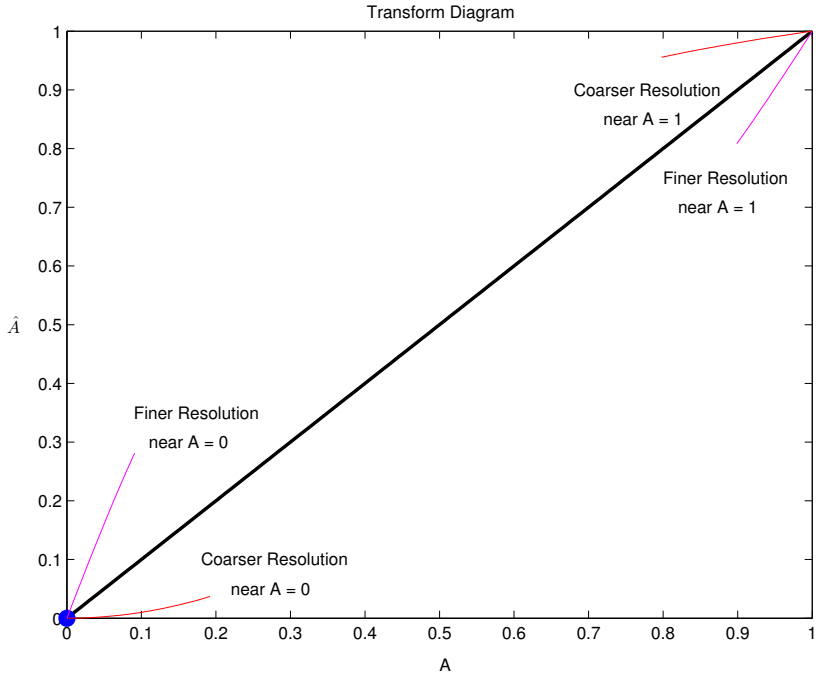

Figure 12: A general idea

The following holds true for the mapping g except on the range $[-1, 1]$. The line $A = \hat{A}$

represents no additional transform. In both of the mappings we will discuss this will occur as $c_A \to \infty$ and provides a good check in determining if the mapping is implemented correctly.

Examining what occurs to a transform near $A = 0$ it can be seen that if the mapping, f, is below the line $A = \hat{A}$ then points that are farther apart in A move closer together in $\hat{A}$. This implies that when collocation points determined in $\hat{A}$ will be spread farther apart in A resulting in a coarser grid. Likewise if f is above the line $A = \hat{A}$, the result is a finer grid close to $A = 0$.

Examining the region $A = 1$, we can see the opposite occurs. If f is above the line $A = \hat{A}$ then points in A that are far apart get mapped closer together in $\hat{A}$. This implies the collocation points determined in $\hat{A}$ are again spread farther apart when mapped back to A, resulting in a coarser grid. Likewise f being below the line results in a finer resolution closer to $A = 1$.

$A = 1$ corresponds to spatial infinity while $A = 0$ corresponds to the line connecting the two black holes. The error decreases as A goes from 0 to 1. Transforms which result in a finer resolution near $A = 0$ and a coarser resolution near $A = 1$ will be discussed. In the B direction the blacks holes are located at $B = \pm 1$. Depending on the relative puncture mass a transform may be sought which concentrates collocation points closer to both black holes simultaneously or possibly towards one black hole and away from the other.

Two transforms will now be looked at. The idea behind both of these transforms is to concentrate collocation points closer to either the black hole that is providing (more/less) of the mass, transform I, or both black holes, transform II. In both cases we wish to concentrate points in the A direction closer to $A = 0$. Both transforms map $[0, 1] \to [0, 1]$ ($[-1, 1] \to [-1, 1]$) in a one-to-one fashion.

10 Transform I

The first transform has following form

$$A = \frac{(c_A^2 - 1)\alpha}{c_A^2 - \alpha^2}, \tag{10.1}$$

$$\frac{B+1}{2} = \frac{(c_B^2 - 1)\frac{(\beta+1)}{2}}{c_B^2 - \frac{(\beta^2+1)^2}{4}}, \tag{10.2}$$

with $c_A > 1$. Since $\alpha \in [0, 1]$, $\alpha^2 \leq \alpha$ and $c_A^2\alpha \leq c_A^2$. Therefore $c_A^2\alpha - \alpha \leq c_A^2 - \alpha^2$. The following inequality holds: $\alpha^2 \leq 1 \leq c_A^2$ so both $(c_A^2 - 1)\alpha$ and $c_A^2 - \alpha^2$ are positive. It can now be concluded that

$$0 \leq \frac{(c_A^2 - 1)\alpha}{c_A^2 - \alpha^2} \leq 1.$$

Taking the derivative of A with respect to α, we find

$$\frac{\mathrm{d}A}{\mathrm{d}\alpha} = \frac{(c_A^2 - 1)(c_A^2 + \alpha^2)}{(c_A^2 - \alpha^2)^2}.$$

This is always greater than 0 so the function is monotonically increasing. Therefore the transform in A maps the closed interval $[0, 1]$ to itself in a one-to-one fashion. Similar analysis can be done on B to see that it maps the interval $[-1, 1]$ to itself in a one-to-one fashion as well.

The inverse transforms are

$$\alpha = \frac{-(c_A^2 - 1) + \sqrt{(c_A^2 - 1)^2 + 4c_A^2 A^2}}{2A}, \tag{10.3}$$

$$\beta = 2\left(\frac{-(c_B^2 - 1) + \sqrt{(c_B^2 - 1)^2 + c_B^2 (B+1)^2}}{B+1}\right) - 1. \tag{10.4}$$

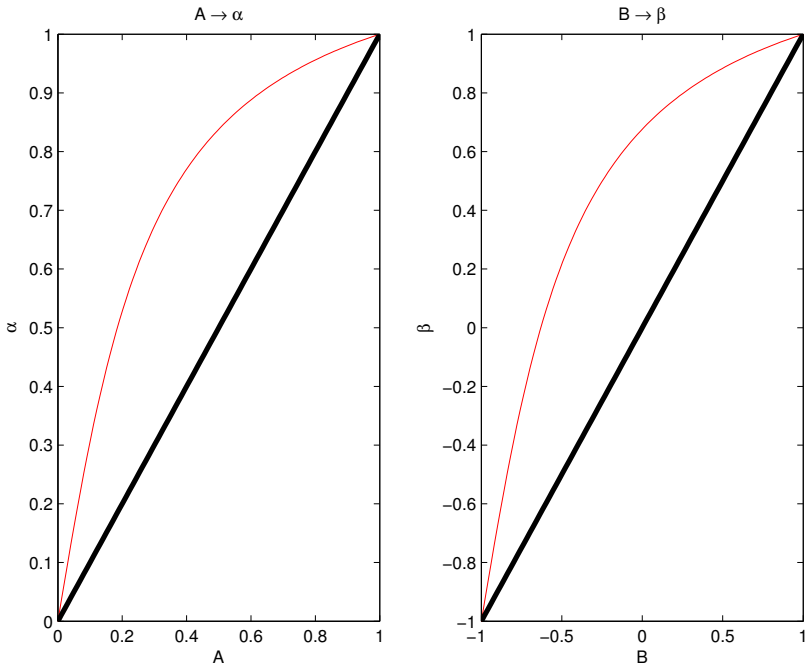

Figure 13: Visualization for the first transform with $c_A = c_B = 1.2$

10.1 The Laplacian

Without the additional transform the Laplacian was calculated to have the from of equation (6.1), repeated here

$$\triangle = L_{AA}\frac{\partial^2}{\partial A^2} + L_A\frac{\partial}{\partial A} + L_{BB}\frac{\partial^2}{\partial B^2} + L_B\frac{\partial}{\partial B} + L_{\phi\phi}\frac{\partial^2}{\partial \phi^2}.$$

Because A is now a function of α (B of β) the partial derivatives in the Laplacian have to be calculated using the chain rule. We will define $\hat{\beta} = \frac{\beta+1}{2}$. The first derivatives are as follows

$$\frac{\mathrm{d}A}{\mathrm{d}\alpha} = \frac{(c_A^2-1)(c_A^2+\alpha^2)}{(c_A^2-\alpha^2)^2},$$

$$\frac{\mathrm{d}B}{\mathrm{d}\beta} = \frac{(c_B^2-1)(c_B^2+\hat{\beta}^2)}{(c_B^2-\hat{\beta}^2)}.$$

We can now determine the partial derivatives of a function f with respect to A and B.

$$\frac{\partial f}{\partial A} = \frac{\partial \alpha}{\partial A}\frac{\partial f}{\partial \alpha} = \left(\frac{\partial A}{\partial \alpha}\right)^{-1}\frac{\partial f}{\partial \alpha} = \frac{(c_A^2-\alpha^2)^2}{(c_A^2-1)(c_A^2+\alpha^2)}\frac{\partial f}{\partial \alpha},$$

$$\frac{\partial f}{\partial B} = \left(\frac{\partial B}{\partial \beta}\right)^{-1}\frac{\partial f}{\partial \beta} = \frac{(c_B^2-\hat{\beta}^2)^2}{(c_B^2-1)(c_B^2+\hat{\beta}^2)}\frac{\partial f}{\partial \beta},$$

with second partial derivatives

$$\begin{aligned}
\frac{\partial^2 f}{\partial A^2} &= \frac{\partial}{\partial A}\frac{\partial f}{\partial A} = \left(\frac{\partial A}{\partial \alpha}\right)^{-1}\frac{\partial}{\partial \alpha}\left(\frac{\partial f}{\partial A}\right) \\
&= \frac{(c_A^2-\alpha^2)^4}{(c_A^2-1)^2(c_A^2+\alpha^2)^2}\frac{\partial^2 f}{\partial \alpha^2} + \frac{2\alpha(c_A^2-\alpha^2)^2(\alpha^4+2c_A^2\alpha^2-3c_A^4)}{(c_A^2-1)^2(c_A^2+\alpha^2)^3}\frac{\partial f}{\partial \alpha}, \\
\frac{\partial^2 f}{\partial B^2} &= \frac{\partial}{\partial B}\frac{\partial f}{\partial B} = \left(\frac{\partial B}{\partial \beta}\right)^{-1}\frac{\partial}{\partial \beta}\left(\frac{\partial f}{\partial B}\right) \\
&= \frac{(c_B^2-\hat{\beta}^2)^4}{(c_B^2-1)^2(c_B^2+\hat{\beta}^2)^2}\frac{\partial^2 f}{\partial \beta^2} + \frac{\hat{\beta}(c_B^2-\hat{\beta}^2)^2(\hat{\beta}^4+2c_B^2\hat{\beta}^2-3c_B^4)}{(c_B^2-1)^2(c_B^2+\hat{\beta}^2)^3}\frac{\partial f}{\partial \beta}.
\end{aligned}$$

We can now determine the Laplacian by substituting these partials into equation (6.1).

10.2 Results

The numerical results can be seen in Figures 14 through 17. In these figures the parameters of the system are given by $c_A = 1000$ and $c_B = 5$. The black hole with the greater puncture mass is located at $(0.5, 0, 0)$ while the other is located at $(-0.5, 0, 0)$.

We can see the collocation points have been shifted towards the black hole located at $(0.5, 0, 0)$. The result is a system where the error is lowered as we consider regions closer to this black hole. The trade off is a raising of error in the other regions, particularly close to the black hole located at $(-0.5, 0, 0)$. In the case where the black holes have different puncture masses this results in a lowering of the overall error and maximum error. When we examine the black holes with similar puncture masses (Figures 14 and 15) we see the maximum error was raised.

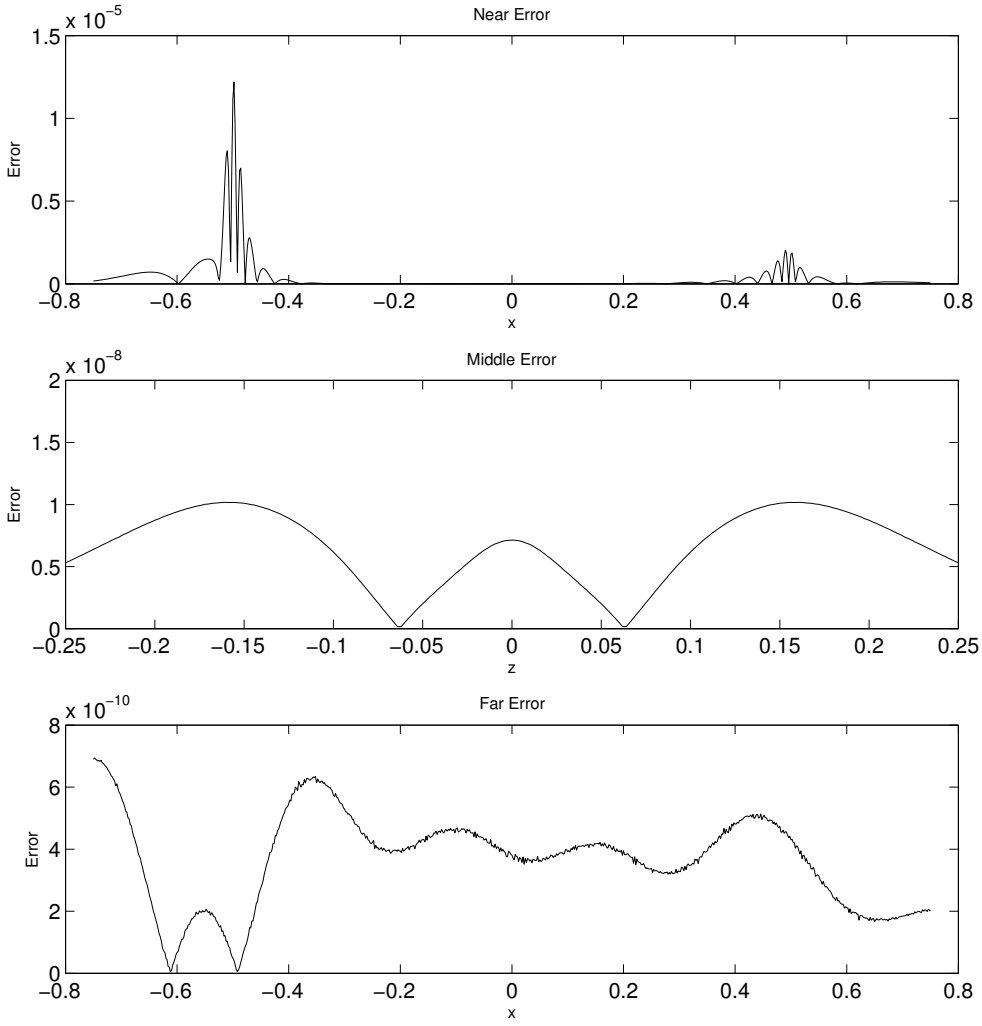

Figure 14: The error for a binary black hole system with $m_1 = m_2 = \frac{1}{3}$, $P_1 = (0, 0.05, 0)$, $P_2 = (0, -0.05, 0)$, $S_1 = S_2 = \vec{0}$.

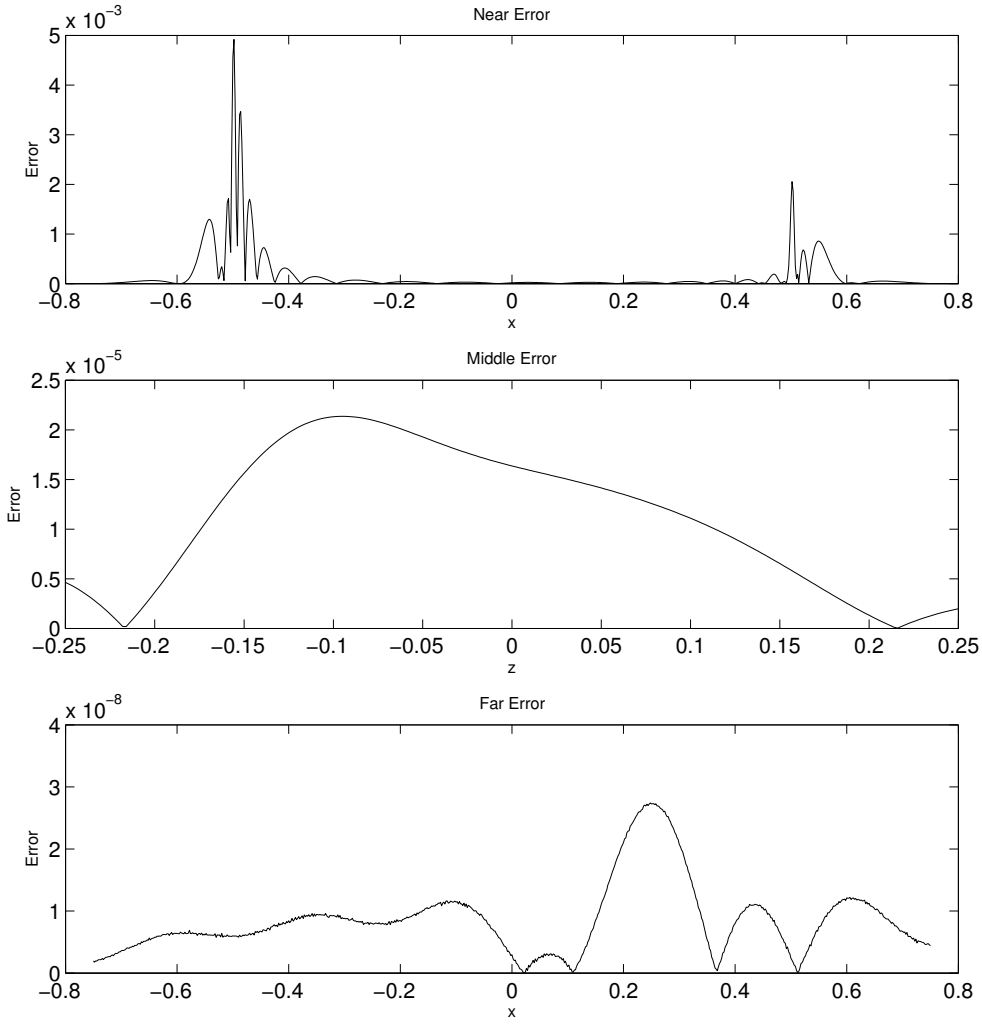

Figure 15: The error for a binary black hole system with $m_1 = m_2 = \frac{1}{3}$, $P_1 = (0, 0.05, 0)$, $P_2 = (0, -0.05, 0)$, $S_1 = (0.03, 0.03, 0.03)$, $S_2 = (0, 0, 0.05)$.

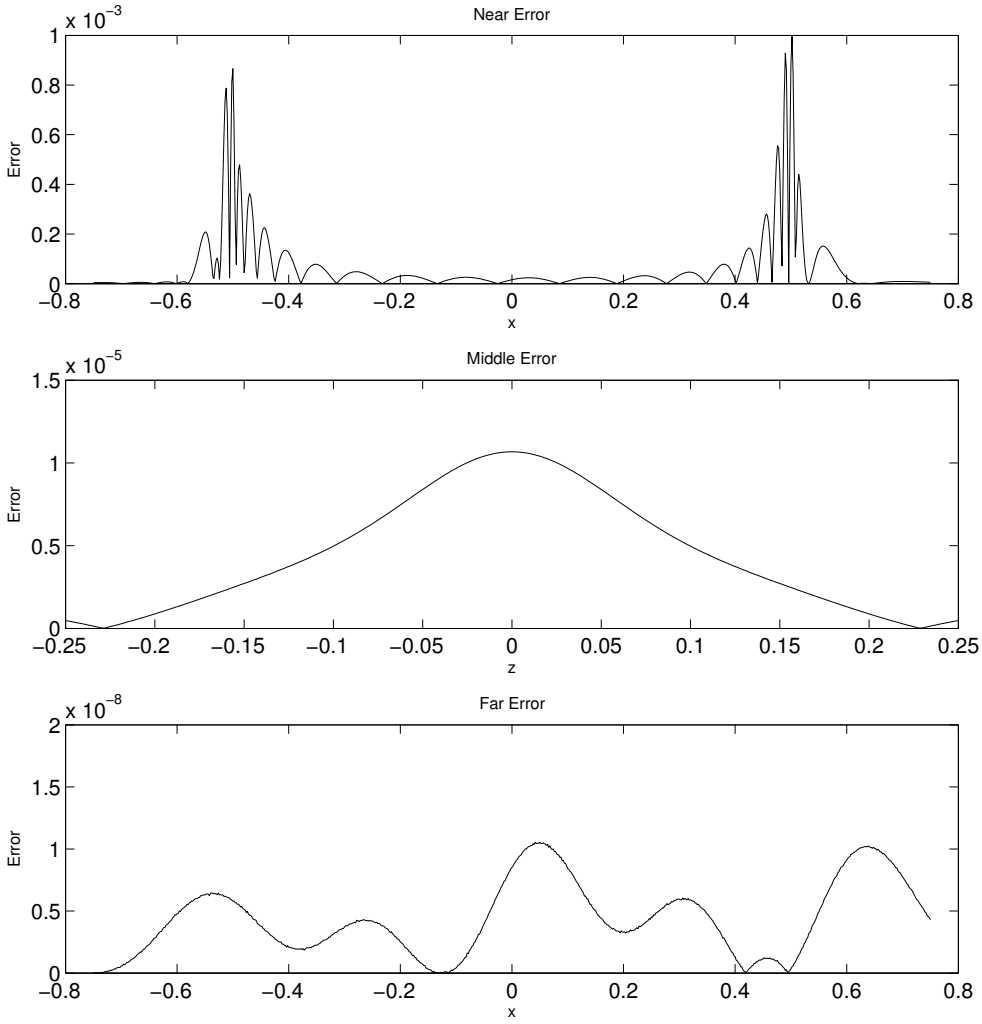

Figure 16: The error for a binary black hole system with $m_1 = 0.4$, $m_2 = 0.1$, $P_1 = (0, 0.05, 0)$, $P_2 = (0, -0.05, 0)$, $S_1 = (0, 0, 0.05)$, $S_2 = \vec{0}$.

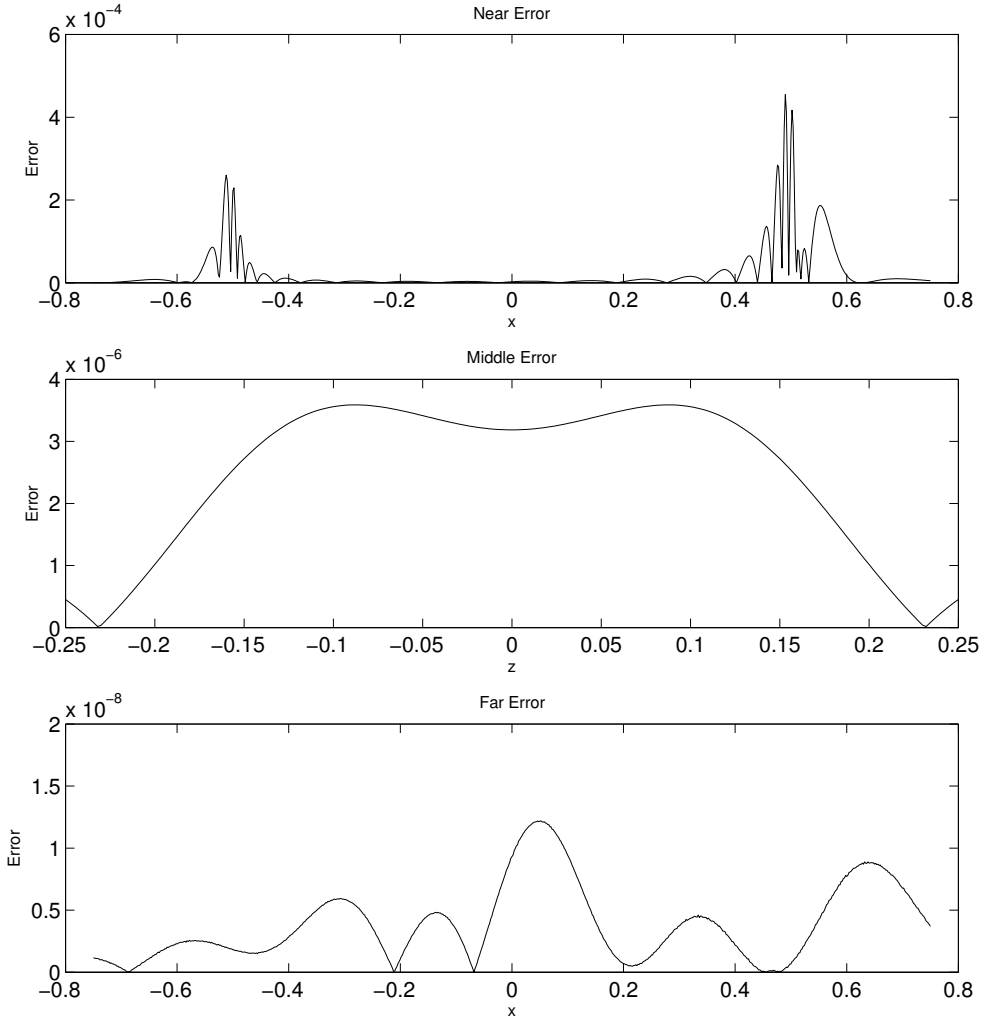

Figure 17: The error for a binary black hole system with $m_1 = 0.4$, $m_2 = 0.1$, $P_1 = P_2 = \vec{0}$, $S_1 = (0, 0, 0.05)$, $S_2 = \vec{0}$.

11 Transform II

The first transform discussed accomplished two things: sent points closer to $A = 0$ (farther from $A = 1$) and closer to $B = -1$ (farther from $B = 1$). This resulted in a finer mesh near both black holes in the A direction but a coarser mesh in the B direction near the black hole located at $B = 1$ and a finer mesh near the black hole located at $B = -1$. We will now examine a transform that results in a finer mesh near both black holes.

The transform in the A direction will remain the same, namely

$$A = \frac{(c_A^2 - 1)\alpha}{c_A^2 - \alpha^2}.$$

In the B direction the following transform will be used

$$B = c_B \arctan\left(\beta \tan\left(\frac{1}{c_B}\right)\right), \tag{11.1}$$

with $c_B > 2/\pi$. This condition must be enforced because $\tan(1/c_B)$ repeats and we only want to look at the principle domain of the tangent function. We can see this transform sends 1 to 1 and -1 to -1.

$$B(1) = c_B \arctan\left(\tan\left(\frac{1}{c_B}\right)\right) = \frac{c_B}{c_B} = 1$$
$$B(-1) = c_B \arctan\left(-\tan\left(\frac{1}{c_B}\right)\right) = -\frac{c_B}{c_B} = -1.$$

The arctangent function is a monotonically increasing function on a bounded domain, therefore the transform maps the region $[-1, 1]$ in a one-to-one fashion onto $[-1, 1]$.

The inverse transform is defined as follows

$$\beta = \frac{\tan\left(\frac{B}{c_B}\right)}{\tan\left(\frac{1}{c_B}\right)}.$$

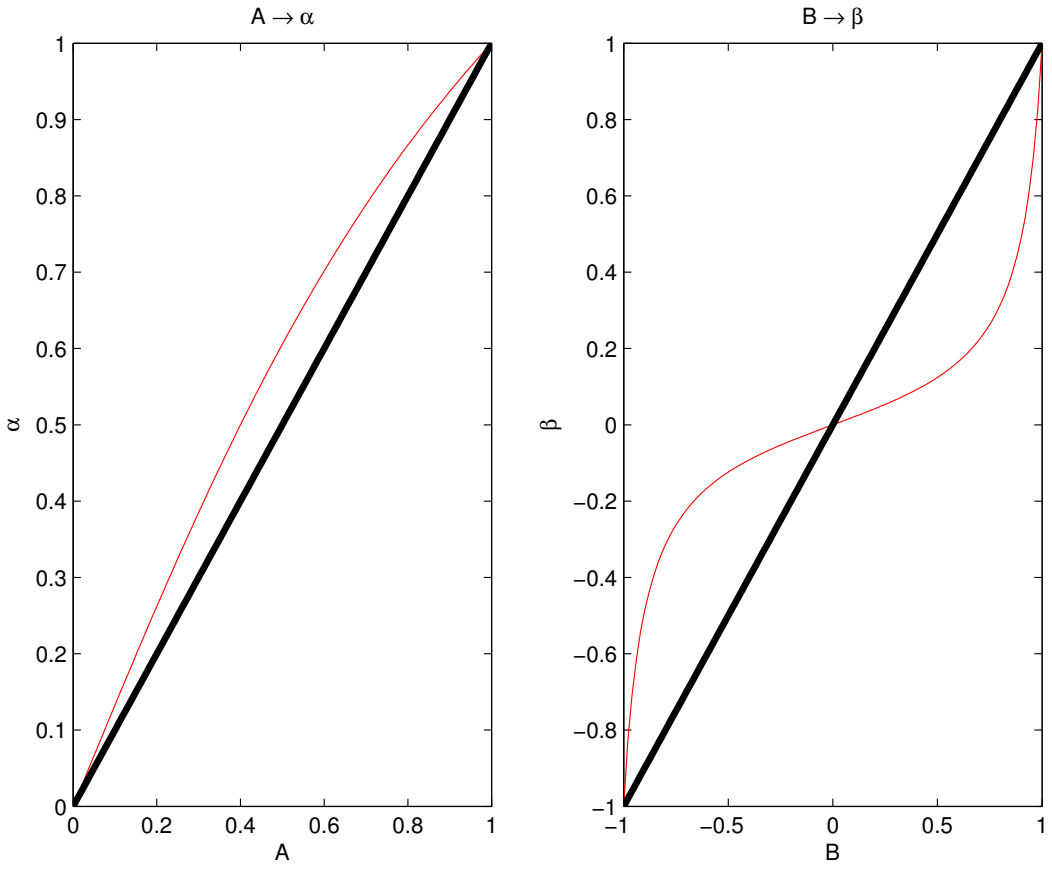

Figure 18: Visualization of the second transform when $c_B = 0.7$ and $c_A = 2$.

11.1 The Laplacian

The Laplacian has to now be calculated in the new coordinate system. In the A direction the partial derivatives are the same as in the first transform. The first derivative for the B direction is

$$\frac{\mathrm{d}B}{\mathrm{d}\beta} = \frac{c_B T}{1+\beta^2 T^2},$$

where $T = \tan\left(\frac{1}{c_B}\right)$. We can now determine the partial derivatives of a function f with respect to B.

$$\frac{\partial f}{\partial B} = \frac{1+\beta^2 T^2}{c_B T}\frac{\partial f}{\partial \beta}$$

and second partial derivatives

$$\begin{aligned}\frac{\partial^2 f}{\partial B^2} &= \frac{\partial}{\partial B}\frac{\partial f}{\partial B} = \left(\frac{\partial B}{\partial \beta}\right)^{-1}\frac{\partial}{\partial \beta}\left(\frac{\partial f}{\partial B}\right) \\ &= \left(\frac{1+\beta^2 T^2}{c_B T}\right)^2 \frac{\partial^2 f}{\partial \beta^2} + \left(\frac{2\beta T(1+\beta^2 T^2)}{c_B^2 T}\right)\frac{\partial f}{\partial \beta}\end{aligned}$$

11.2 Results

The numerical results can be seen in Figures 19 through 22. In these figures the parameters

of the system are given by $c_A = 1000$ and $c_B = 5$. The black hole with the greater puncture mass is located at $(0.5, 0, 0)$, while the other is located at $(-0.5, 0, 0)$.

This method does not lower the overall error, or maximum error, in any case for the near section. Instead it keeps the error relatively similar to the original untransformed system. One interesting area for further research would be to develop a transform that is based off of the relative masses of the two black holes to determine the coefficients for the system and how much of each transform should be applied.

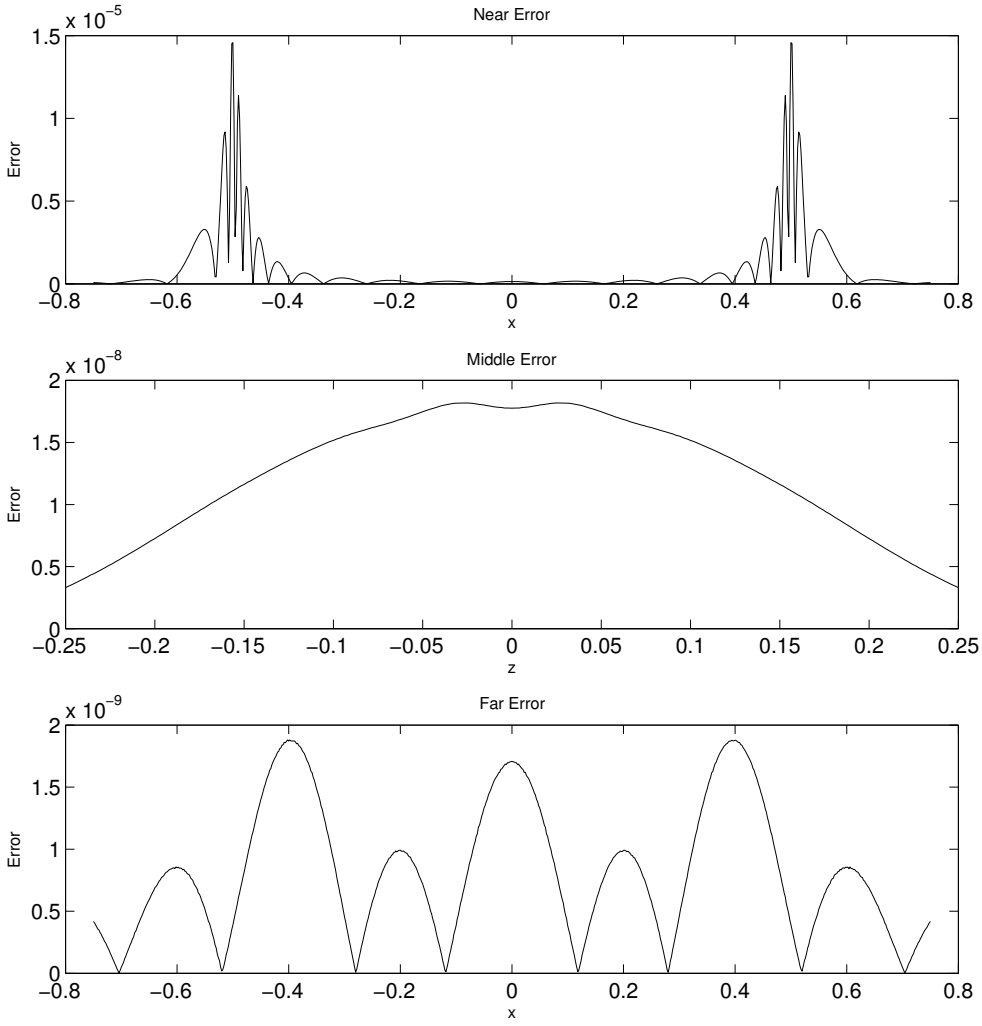

Figure 19: The error for a binary black hole system with $m_1 = m_2 = \frac{1}{3}$, $P_1 = (0, 0.05, 0)$, $P_2 = (0, -0.05, 0)$, $S_1 = S_2 = \vec{0}$.

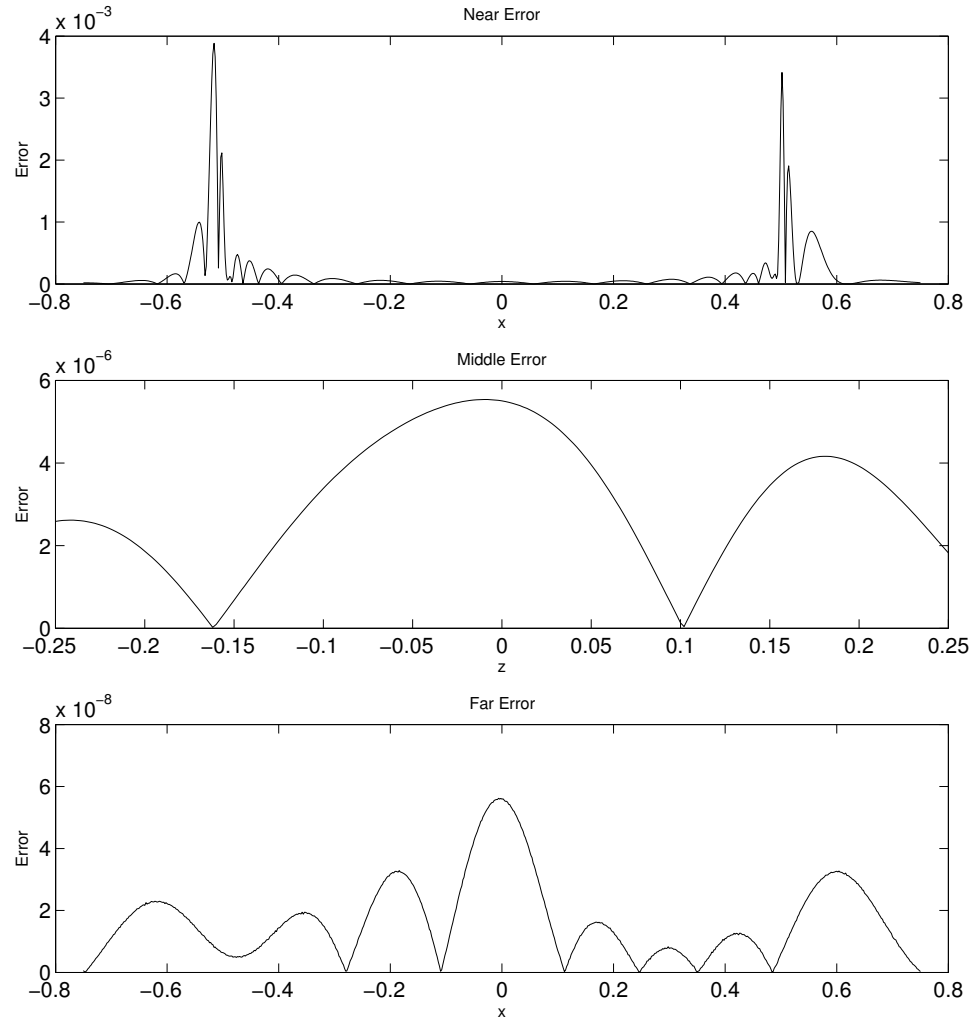

Figure 20: The error for a binary black hole system with $m_1 = m_2 = \frac{1}{3}$, $P_1 = (0, 0.05, 0)$, $P_2 = (0, -0.05, 0)$, $S_1 = (0.03, 0.03, 0.03)$, $S_2 = (0, 0, 0.05)$.

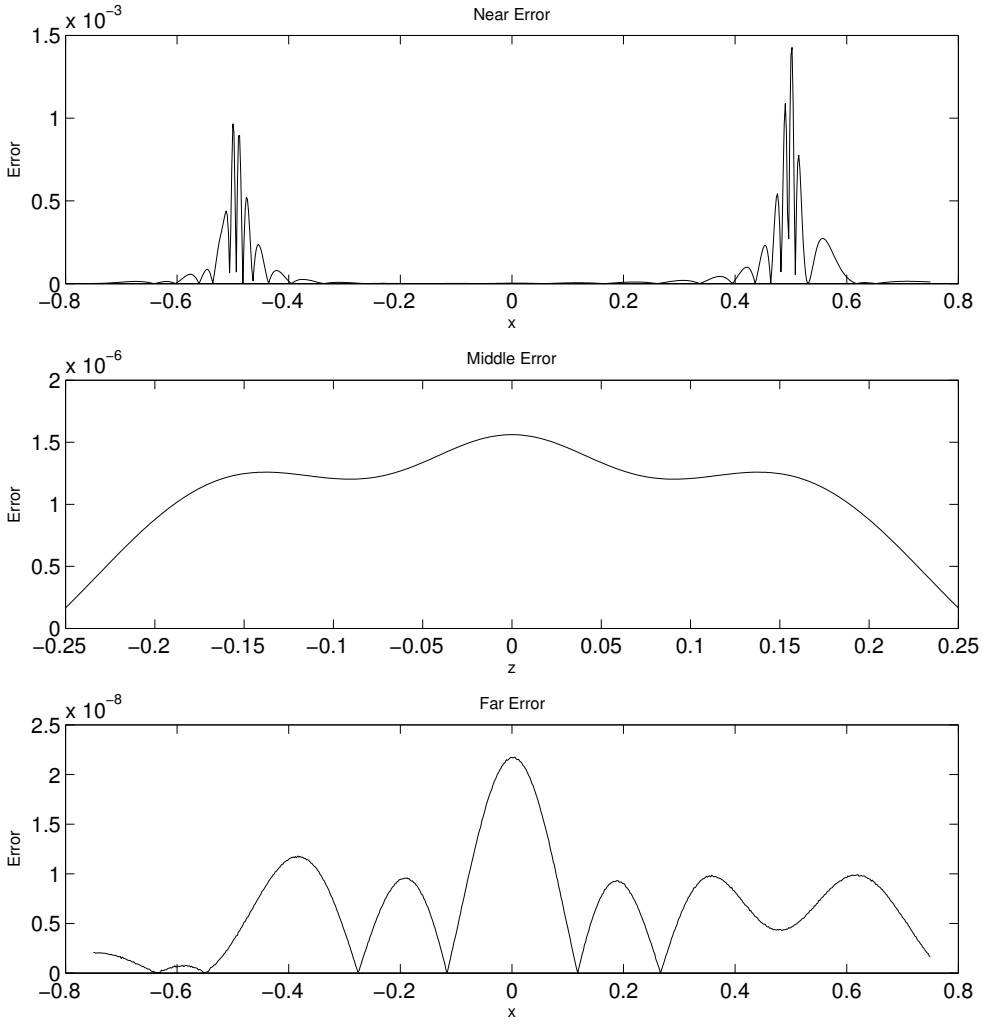

Figure 21: The error for a binary black hole system with $m_1 = 0.4$, $m_2 = 0.1$, $P_1 = (0, 0.05, 0)$, $P_2 = (0, -0.05, 0)$, $S_1 = (0, 0, 0.05)$, $S_2 = \vec{0}$.

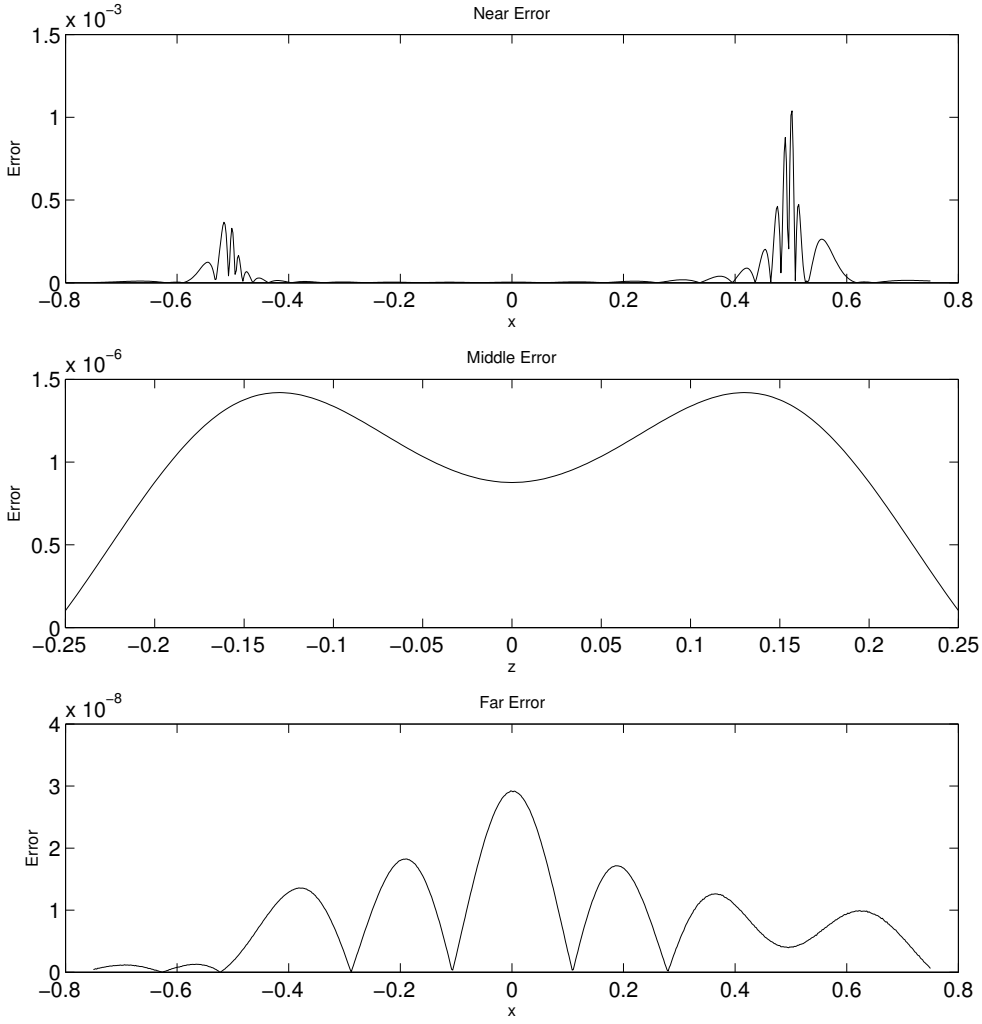

Figure 22: The error for a binary black hole system with $m_1 = 0.4$, $m_2 = 0.1$, $P_1 = P_2 = \vec{0}$, $S_1 = (0, 0, 0.05)$, $S_2 = \vec{0}$.

A Properties of Chebyshev Polynomials

Chebyshev Polynomials of the first kind are defined in two ways,

$$T_n(x) = \cos(n \arccos(x)),$$

or recursively

$$T_n(x) = 2xT_{n-1}(x) - T_{n-2}; \qquad n = 2, 3, 4, \ldots$$

$$T_0(x) = 1; \quad T_1(x) = x.$$

Chebyshev Polynomials of the second kind are defined as

$$U_n(x) = \frac{\sin((n+1)\arccos(x))}{\sin(\arccos(x))}.$$

The derivatives of the Chebyshev polynomials are

$$\frac{\mathrm{d}T_n}{\mathrm{d}x} = nU_{n-1},$$

$$\frac{\mathrm{d}^2T_n}{\mathrm{d}x^2} = n\frac{(n+1)T_n - U_n}{x^2 - 1}.$$

The extrema of $T_n(x)$ are

$$x_k = \cos\left(\frac{\left(k + \frac{1}{2}\right)\pi}{n}\right); \qquad 0 \le k \le n-1.$$

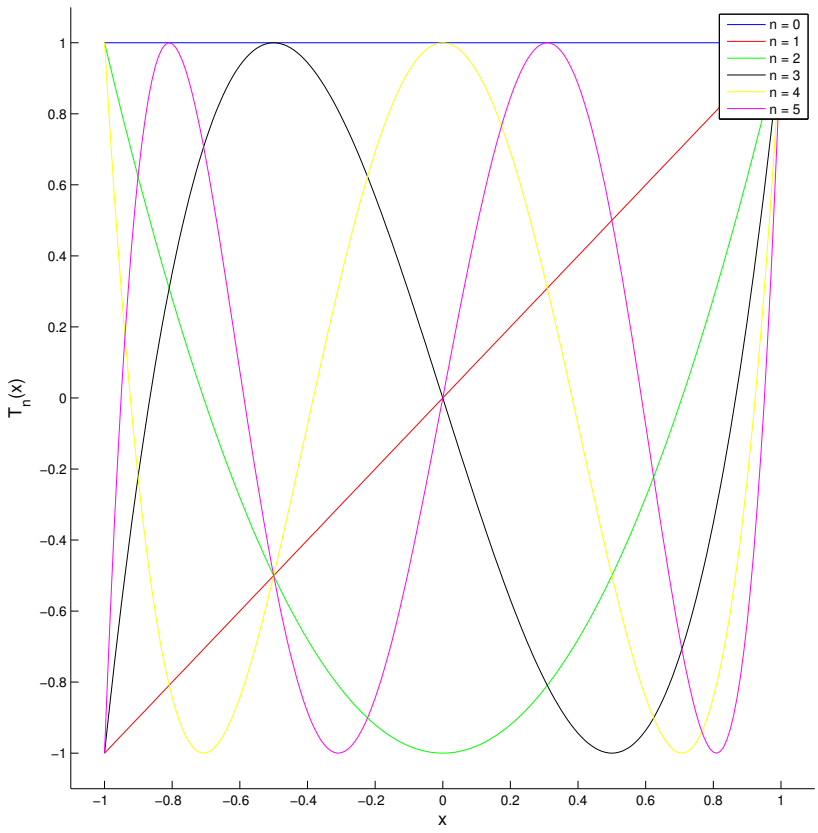

Figure 23: The first six Chebyshev polynomials.

This leads to the discrete orthogonality property:

$$\sum_{k=0}^{n-1} T_i(x_k)T_j(x_k) = \begin{cases} 0; & i \neq j \\ n; & i = j = 0 \\ \frac{n}{2}; & i = j \neq 0 \end{cases}$$

Suppose that $f(x) \approx \sum_{j=1}^{n-1} c_j T_j(x)$ then

$$\sum_{k=0}^{n-1} f(x_k)T_j(x_k) = \sum_{k=0}^{n-1} c_i T_i(x_k)T_j(x_k) = \begin{cases} 0; & i \neq j \\ nc_0: & i = j = 0 \\ \frac{nc_i}{2}: & i = j \neq 0 \end{cases}$$

Inverting this result we can solve for the coefficients;

$$c_0 = \frac{1}{n} \sum_{k=0}^{n-1} f(x_k)$$
$$c_i = \frac{2}{n} \sum_{k=0}^{n-1} f(x_k)T_i(x_k)$$

B Einstein Notation

In Einstein notation, when an index appears twice it implies a summation over all values of the index. The expression $c_i x^i$ is equivalent to $c_1 x^1 + c_2 x^2 + c_3 x^3$. Upper indices correspond to the indices of the coordinate system, contravariant, while lower indices are linear operations on the coordinates, covariant.

Latin letters represent spatial coordinates only and take on the values $1, 2, 3$, corresponding to the standard x, y, z. Greek letters correspond to space time coordinates and take on the values $0, 1, 2, 3$ where x^0 represents the time dimension and the others correspond to i, j, k as before.

For example, in Einstein notation $u_i v^i$ corresponds to $u_1 v^1 + u_2 v^2 + u_3 v^3$, and can be seen as the inner (or dot) product of the vectors $\vec{u}$, $\vec{v}$. The outer product of the two vectors, $\vec{u}$ and $\vec{v}$, is represented as $u^i v^i$ and yields a 3x3 matrix.

The momentum constraints pertaining to black holes, which arise in general relativity, can be represented in a nice compact form using Einstein notation,

$$\nabla_a K^{ab} = \begin{cases} \nabla_1 K^{11} + \nabla_2 K^{21} + \nabla_3 K^{31} \\ \nabla_1 K^{12} + \nabla_2 K^{22} + \nabla_3 K^{32} \quad = 0 \\ \nabla_1 K^{13} + \nabla_2 K^{23} + \nabla_3 K^{33} \end{cases}$$

C The Inverse of the Compactification Scheme

When obtaining a solution at a specific point, or grid, in the standard cartesian the coordinates of the transform described in Section 5 must be inverted. The transform from (x, y, z) to (A, B, ϕ) will now be discussed.

Using the coordinate transform obtained before

$$x = b\cosh(\xi)\cos(\eta), \tag{C.1}$$

$$\rho = b\sinh(\xi)\sin(\eta). \tag{C.2}$$

We will now solve for A, B and ϕ through a few steps. First we will say that $\hat{x} = \frac{x}{b}$ and $\hat{\rho} = \frac{\rho}{b}$. From equations (C.1) and (C.2) we obtain

$$\frac{\hat{x}}{\cosh(\xi)} = \cos(\eta), \qquad \frac{\hat{\rho}}{\sinh(\xi)} = \sin(\eta). \tag{C.3}$$

We can use this result with the Pythagorean theorem for sines and cosines to obtain

$$\begin{aligned} 1 &= \frac{\hat{x}^2}{\cosh^2(\xi)} + \frac{\hat{\rho}^2}{\sinh^2(\xi)} \\ &= \frac{\hat{x}^2}{\cosh^2(\xi)} + \frac{\hat{\rho}^2}{\cosh^2(\xi) - 1}. \end{aligned} \tag{C.4}$$

One more substitution will be made: $u = \cosh^2\xi$. Equation (C.4) can now be written as a quadratic in u,

$$u^2 - u(1 + \hat{x}^2 + \hat{\rho}^2) + \hat{x}^2 = 1, \tag{C.5}$$

and can be solved using the quadratic equation to obtain the solution for u.

$$u = \frac{1}{2}\left[1 + \hat{x}^2 + \hat{\rho}^2 \pm \sqrt{(1 + \hat{x}^2 + \hat{\rho}^2)^2 - 4\hat{x}^2}\right]. \tag{C.6}$$

Since $u = \cosh^2(\xi)$, u must be greater than or equal to 1. The discriminant of equation (C.5) will be examined to determine if the positive or the negative should be used. It can never be negative so two cases will be examined, when the discriminant is greater than 0 and when it equals 0.

The discriminant is equal to 0 only when $x = \pm 1$ and $\rho = 0$. At these points

$$u_+ = u_- = \frac{1}{2}(1 + (\pm 1)^2) = 1.$$

However since $u_+ = u_-$, this does not help in determining which should be used. The case will now be examined when the discriminant is greater than 0. We will first put a lower bound on u_+, the "positive" root. Since the discriminant is positive, this is the minimum u_+ can be occurs at the point $\hat{x} = 0$, $\hat{\rho} = 0$. ($\hat{x}^2$, $\hat{\rho}^2$, $\sqrt{(1 + \hat{x}^2 + \hat{\rho}^2)^2 - 4\hat{x}^2}$ are all greater than 0 for all other values of $\hat{x}$ and $\hat{\rho}$). Therefore

$$
\begin{aligned}
u_+ &= \frac{1}{2}\left[1+\hat{x}^2+\hat{\rho}^2+\sqrt{(1+\hat{x}^2+\hat{\rho}^2)^2-4\hat{x}^2}\right] \\
&\geq \frac{1}{2}\left[1+\sqrt{1^2}\right] \\
&= 1.
\end{aligned} \tag{C.7}
$$

We will now put an upper bound on the smaller root, u_-. We will first note because ρ is a real number, $-\hat{\rho}^2 \leq \hat{\rho}^2$ therefore $-2\hat{\rho}^2 \leq 2\hat{\rho}^2$. Adding the same thing to both sides keeps the equality the same,

$$
\begin{aligned}
\hat{x}^4+\hat{\rho}^4+2\hat{x}^2\hat{\rho}^2-2\hat{x}^2-2\hat{\rho}^2+1 &\leq \hat{x}^4+\hat{\rho}^4+2\hat{x}^2\hat{\rho}^2-2\hat{x}^2+2\hat{\rho}^2+1, \\
(\hat{x}^2+\hat{\rho}^2-1)^2 &\leq (\hat{x}^2+\hat{\rho}^2+1)^2-4\hat{x}^2, \\
\hat{x}^2+\hat{\rho}^2-1 &\leq \sqrt{(\hat{x}^2+\hat{\rho}^2+1)^2-4\hat{x}^2}, \\
1+\hat{x}^2+\hat{\rho}^2-\sqrt{(\hat{x}^2+\hat{\rho}^2+1)^2-4\hat{x}^2} &\leq 2,
\end{aligned}
$$

$$
\begin{aligned}
u_- &= \frac{1}{2}\left[1+\hat{x}^2+\hat{\rho}^2-\sqrt{(1+\hat{x}^2+\hat{\rho}^2)^2-4\hat{x}^2}\right] \\
&\leq \frac{2}{2} = 1.
\end{aligned} \tag{C.8}
$$

Since the smaller root is always less than one and the larger root always greater than one, the solution for u is

$$
u = \frac{1}{2}\left[1+\hat{x}^2+\hat{\rho}^2+\sqrt{(1+\hat{x}^2+\hat{\rho}^2)^2-4\hat{x}^2}\right]. \tag{C.9}
$$

A can now be determined

$$\xi = \operatorname{arccosh}(\sqrt{u}), \qquad A = \tanh\left(\frac{\xi}{2}\right). \tag{C.10}$$

We will now solve for B in almost the same way. Starting with Equations (C.1) and (C.2) we can say

$$\frac{\hat{x}}{\cos(\eta)} = \cosh(\xi), \qquad \frac{\hat{\rho}}{\sin(\eta)} = \sinh(\xi). \tag{C.11}$$

Using the identity $\cosh^2(x) + \sinh^2(x) = 1$,

$$\begin{aligned} 1 &= \frac{\hat{x}^2}{\cos^2(\eta)} + \frac{\hat{\rho}^2}{\sin^2(\eta)} \\ &= \frac{\hat{x}^2}{\cos^2(\eta)} + \frac{\hat{\rho}^2}{1-\cos^2(\eta)} \end{aligned} \tag{C.12}$$

We will now solve for $v = \cos^2(\eta)$. As before Equation (C.12) can now be written as a quadratic in v and a solution can be obtained by using the quadratic equation.

$$v^2 - v(1 + \hat{x}^2 + \hat{\rho}^2) + \hat{x}^2 = 0. \tag{C.13}$$

with solution

$$v = \frac{1}{2}\left[1 + \hat{x}^2 + \hat{\rho}^2 \pm \sqrt{(1 + \hat{x}^2 + \hat{\rho}^2)^2 - 4\hat{x}^2}\right].$$

Since $v = \cos^2(\eta)$, v must be less than or equal to 1. The quadratic in v is the same as the quadratic in u, so the same analysis applies. Therefore

$$v = \frac{1}{2}\left[1 + \hat{x}^2 + \hat{\rho}^2 - \sqrt{\left(1 + \hat{x}^2 + \hat{\rho}^2\right)^2 - 4\hat{x}^2}\right]. \tag{C.14}$$

B can now be determined

$$\eta = \arccos(\sqrt{v}), \qquad B = \tan\left(\frac{1}{2}\left(\eta - \frac{\pi}{2}\right)\right). \tag{C.15}$$

References

[1] Marcus Ansorg, Bernd Brugmann, and Wolfgang Tichy. Single-domain spectral method for black hole puncture data. *The American Physical Society*, September 2004.

[2] Thomas W. Baumgarte and Stuart L. Shapiro. Binary black hole mergers. *Physics Today*, October 2011.

[3] John P. Boyd. *Chebyshev and Fourier Spectral Methods.* Dover Publications, Inc., Mineola, New York, 2000.

[4] Steven Brandt and Bernd Brugmann. A simple construction of initial data for multiple black holes. *Phys. Rev. Lett.*, February 1997.

[5] Joshua A. Faber and Frederic A. Rasio. Binary neutron star mergers. *Living Reviews in Relativity*, July 2012.